30. Hayakawa Y, Berzins SP, Crowe NY, Godfrey DI, Smyth MJ. Antigen-induced tolerance by intrathymic modulation of self-recognizing inhibitory receptors. Nat Immunol. 2004;5:590-596.
31. Carnaud C, Lee D, Donnars O, et al. Cross-talk between cells of the innate immune system: NKT cells rapidly activate NK cells. J Immunol. 1999; 163:4647-4650.
32. Soloski MJ, DeCloux A, Aldrich CJ, Forman J. Structural and functional characteristics of the class Ib molecule, Qa-1. Immunol Rev. 1995;147: 67-89.
33. Aldrich CJ, DeCloux A, Woods AS, Cotter RJ, Soloski MJ, Forman J. Identification of a Tap-dependent leader peptide recognized by alloreactive T cells specific for a class Ib antigen. Cell. 1994;79: 649-658.
34. Vivier E, Anfossi N. Inhibitory NK-cell receptors on T cells: witness of the past, actors of the future. Nat Rev Immunol. 2004;4:190-198.
35. Maeda M, Lohwasser S, Yamamura T, Takei F. Regulation of NKT cells by Ly49: analysis of primary NKT cells and generation of NKT cell line. J Immunol. 2001;167:4180-4186.
36. Takeda K, Hayakawa Y, Van Kaer L, Matsuda H, Yagita H, Okumura K. Critical contribution of liver natural killer T cells to a murine model of hepatitis. Proc Natl Acad Sci U S A. 2000;97:5498-5503.
37. Osman Y, Kawamura T, Naito T, et al. Activation of hepatic NKT cells and subsequent liver injury following administration of α-galactosylceramide. Eur J Immunol. 2000;30:1919-1928.
38. Ito K, Karasawa T, Kawano T, et al. Involvement of decidual Vα14 NKT cells in abortion. Proc Natl Acad Sci U S A. 2000;97:740-744.
39. Tupin E, Nicoletti A, Elhage R, et al. CD1d-dependent activation of NKT cells aggravates atherosclerosis. J Exp Med. 2004;199:417-422.
40. Hu D, Ikizawa K, Lu L, Sanchirico ME, Shonohara ML, Cantor H. Analysis of regulatory CD8 T cells in Qa-1-deficient mice. Nat Immunol. 2004;5:516-523.
41. Schümann J, Voyle RB, Wei BY, MacDonald HR. Influence of the TCR Vβ domain on the avidity of CD1d:α-galactosylceramide binding by invariant Vα 14 NKT cells. J Immunol. 2003;170:5815-5819.
42. Giaccone G, Punt CJ, Ando Y, et al. A phase I study of the natural killer T-cell ligand α-galactosylceramide (KRN7000) in patients with solid tumors. Clin Cancer Res. 2002;8:3702-3709.
43. Nieda M, Okai M, Tazbirkova A, et al. Therapeutic activation of $V\alpha24^+V\beta11^+$ NKT cells in human subjects results in highly coordinated secondary activation of acquired and innate immunity. Blood. 2004;103:383-389.
44. Mars LT, Novak J, Liblau RS, Lehuen A. Therapeutic manipulation of iNKT cells in autoimmunity: modes of action and potent risks. Trends Immunol. 2004;25:471-476.

ARTHRITIS & RHEUMATISM
Vol. 52, No. 6, June 2005, pp 1941–1948
DOI 10.1002/art.21056

The Involvement of $V_\alpha 14$ Natural Killer T Cells in the Pathogenesis of Arthritis in Murine Models

Asako Chiba, Shinjiro Kaieda, Shinji Oki, Takashi Yamamura, and Sachiko Miyake

Objective. **To examine the physiologic role of natural killer T (NKT) cells bearing $V_\alpha 14$ T cell receptor (TCR) in the pathogenesis of collagen-induced arthritis (CIA) and antibody-induced arthritis in mice.**

Methods. **NKT cells were stained with α-galactosylceramide–loaded CD1 dimer, and then assessed using flow cytometry. CIA was induced in mice by immunization on days 0 and 21 with type II collagen (CII) emulsified with an equal volume of Freund's complete adjuvant. Anti-CII antibodies were measured by enzyme-linked immunosorbent assay. For antibody-induced arthritis, mice were injected with anti-CII monoclonal antibodies (mAb) followed by lipopolysaccharide, or with serum from KRN TCR–transgenic mice crossed with nonobese diabetic mice (K/BxN). The severity of arthritis was monitored with a macroscopic scoring system.**

Results. **The number of NKT cells increased in the liver at the peak of the clinical course of CIA. Administration of anti-CD1 mAb inhibited development of CIA. The severity of CIA in NKT cell–deficient mice was reduced compared with that in wild-type mice. The IgG1:IgG2a ratio of anti-CII was elevated and production of interleukin-10 from draining lymph node cells was increased in NKT cell–deficient mice. NKT cell–deficient mice were significantly less susceptible to antibody-induced arthritis.**

Conclusion. **NKT cells contribute to the pathogenesis of arthritis by enhancing autoantibody-mediated inflammation. NKT cells also contribute the disease process in a deleterious way, due, at leas part, to the alteration of the Th1/Th2 balance in T response to CII.**

Rheumatoid arthritis (RA) is a common au immune disease characterized by persistent inflam tion of the joints. Affected joints display hyperplasia the synovia with large cellular infiltrates of several types, including neutrophils, macrophages, T cells cells, dendritic cells, and fibroblasts. Complement d osition and high levels of proinflammatory cytok expression are found in the synovial and periartic regions, and the perpetuation of synovitis results destruction of the cartilage and bone of the affec joints. Although the etiology of RA remains contro sial, cumulative evidence suggests that T cell–media autoimmune responses play an important role, and ensuing inflammation is a critical component in processes leading to damage of joint cartilage bone (1).

Natural killer T (NKT) cells are a unique sub of T cells that coexpress receptors of the NK line and α/β T cell receptor (TCR). A majority of N cells express an invariant TCRα chain (encoded b $V_\alpha 14$–$J_\alpha 281$ rearrangement in mice and a homolog $V_\alpha 24$–$J_\alpha Q$ rearrangement in humans). Unlike conv tional T cells that recognize peptides in association w the major histocompatibility complex (MHC), V NKT cells recognize glycolipid antigens such α-galactosylceramide (α-GC) presented by the nonpo morphic MHC class I–like protein, CD1d. $V_\alpha 14$ N cells have been demonstrated to regulate a variety immune responses through their capacity to produc large amount of cytokines, including interleukin-4 (IL and interferon-γ (IFNγ), in response to TCR ligation cytokine stimulation (2–4). Furthermore, we previou demonstrated that stimulation of $V_\alpha 14$ NKT cells w the glycolipid ligand, OCH, can inhibit collagen-indu arthritis (CIA), a murine experimental model for

Supported by a grant-in-aid for scientific research from the Japan Society for the Promotion of Science (B-14370169), the Uehara Memorial Foundation, the Kato Memorial Bioscience Foundation, and the Pharmaceutical and Medical Devices Agency.

Asako Chiba, MD, PhD, Shinjiro Kaieda, MD, Shinji Oki, PhD, Takashi Yamamura, MD, PhD, Sachiko Miyake, MD, PhD: National Institute of Neuroscience, Tokyo, Japan.

Address correspondence and reprint requests to Sachiko Miyake, MD, PhD, Department of Immunology, National Institute of Neuroscience, NCNP 4-1-1 Ogawahigashi, Kodaira, Tokyo 187-8502, Japan. E-mail: miyake@ncnp.go.jp.

Submitted for publication July 30, 2004; accepted in revised form March 1, 2005.

induced by immunization with type II collagen (CII), suggesting that $V_\alpha14$ NKT cells are a potential target for RA therapy (5).

Although the precise function of $V_\alpha14$ NKT cells remains to be elucidated, evidence indicates that $V_\alpha14$ NKT cells play a critical role in the regulation of autoimmune responses (6–8). Abnormalities in the numbers and function of $V_\alpha14$ NKT cells have been observed in patients with autoimmune diseases, including RA, as well as in a variety of mouse strains that are genetically predisposed to the development of autoimmune diseases (9–15). Despite these accumulating data, the role of $V_\alpha14$ NKT cells in the pathogenesis of arthritis still remains unclear.

In the present study, we show that blockade of CD1d results in the amelioration of CIA. In addition, the severity of CIA induced in $V_\alpha14$ NKT cell–deficient mice was reduced in comparison with that in wild-type mice, due to a reduction in the Th1 deviation of T cell responses to CII. Furthermore, mice deficient in $V_\alpha14$ NKT cells were significantly less susceptible to antibody-induced arthritis, indicating that $V_\alpha14$ NKT cells also contribute to autoantibody-mediated inflammation.

MATERIALS AND METHODS

Mice. DBA1/J mice were purchased from Oriental Yeast Co., Ltd (Tokyo, Japan). C57BL/6 (B6) mice were purchased from Clea Laboratory Animal Corporation (Tokyo, Japan). $J_\alpha281$-knockout mice were kindly provided by Dr. Masaru Taniguchi (Riken Research Center for Allergy and Immunology, Yokohama, Japan) (16), and were generated in the 129 strain and backcrossed 10 times to the B6 background. CD1-knockout mice were kindly provided by Dr. Steve B. Balk (Beth Israel Deaconess Medical Center, Harvard Medical School, Boston, MA) (17), and were generated in the 129 strain and backcrossed 7 times to the B6 background. KRN TCR–transgenic mice were kindly provided by Drs. Christophe Benoist and Diane Mathis (Joslin Diabetes Center, Boston, MA) (18). The animals were kept under specific pathogen–free conditions.

Flow cytometric analysis of NKT cells. Cells were prepared from various organs of control DBA1/J mice and CIA mice at 30–35 days after the first immunization. Control mice were injected intradermally with vehicle alone emulsified in Freund's complete adjuvant (CFA) at day 0 and in Freund's incomplete adjuvant (IFA) at day 21. Dimer XI Recombinant Soluble Dimetric Mouse CD1d, fluorescein isothiocyanate–conjugated A85-1 monoclonal antibodies (mAb) (anti-mouse IgG1), and allophycocyanin-conjugated anti-TCRβ chain were purchased from BD Biosciences PharMingen (San Diego, CA). Loading of α-GC to CD1d and staining for Dimer XI were achieved in accordance with the manufacturer's protocol. Flow cytometric analysis was performed with FACSCaliber flow cytometry (Becton Dickinson Immunocytometry Systems, Mountain View, CA).

Induction of CIA. Mice were immunized intradermally at the base of the tail with either 200 μg of bovine CII (for DBA1/J mice) or 100 μg of chicken CII (for B6 mice) (Collagen Research Center, Tokyo, Japan) emulsified with an equal volume of CFA and containing 250 μg of H37Ra *Mycobacterium tuberculosis* (Difco, Detroit, MI). B6 mice received a booster by intradermal injection with the same antigen preparation on day 21. DBA1/J mice received a booster by intradermal injection with 200 μg of bovine CII emulsified with IFA.

Induction of anti-CII antibody–induced arthritis. Mice were injected intravenously with 2 mg of the mixture of anti-CII mAb (Arthrogen-CIA mAb; Chondrex, Seattle, WA), and 3 days later, 50 μg of lipopolysaccharide (LPS) was injected intraperitoneally. Control mice were injected with mouse IgG (Sigma, St. Louis, MO) followed by LPS injection.

Induction of arthritis by K/BxN serum transfer. As previously described, KRN TCR–transgenic mice maintained on the B6 background were crossed with nonobese diabetic (NOD) mice to generate K/BxN mice that develop spontaneous arthritis (18). K/BxN serum pools were prepared from 8-week-old, arthritic mice, and 200 μl of the serum was injected intraperitoneally into the animals to induce arthritis. Sera from nontransgenic littermate mice crossed with NOD mice (BxN) were used as the control.

Clinical assessment of arthritis. Mice were examined for signs of joint inflammation, using the following scoring system: 0 = no change, 1 = significant swelling and redness of 1 digit, 2 = mild swelling and erythema of the limb or swelling of >2 digits, 3 = marked swelling and erythema of the limb, and 4 = maximal swelling and redness of the limb and subsequent ankylosis. The average of the macroscopic score was expressed as the cumulative value of all paws, with a maximum possible score of 16.

In vivo antibody treatment. Anti-CD1–blocking, non–cell-depleting mAb (1B1) was purchased from BD Biosciences PharMingen (19). Mice were treated intraperitoneally with 250 μg of either blocking anti-CD1d mAb or non–isotype-matched whole rat IgG (Sigma) as control, twice per week starting from 21 days after the first immunization with CII.

Measurements of CII-specific IgG1 and IgG2a. Either chicken or bovine CII (1 mg/ml) was coated onto enzyme-linked immunosorbent assay plates (Sumitomo Bakelite, Tokyo, Japan) at 4°C overnight. After blocking with 1% bovine serum albumin in phosphate buffered saline, serially diluted serum samples were added to CII-coated wells. For detection of anti-CII antibodies, the plates were incubated for 1 hour with biotin-labeled anti-IgG1 and anti-IgG2a (Southern Biotechnology Associates, Birmingham, AL) or anti-IgG antibodies (CN/Cappel, Aurora, OH) and then incubated with streptavidin-peroxidase. After adding a substrate, the reaction was evaluated, and antibody titers were calculated on the basis of dilution/absorbance curves.

Cytokine measurement. B6 or $J_\alpha281$-knockout mice were immunized with 100 μg of CII on days 0 and 21. Ten days after the second immunization, the lymph node cells from B6 or $J_\alpha281$-knockout mice were cultured for 48 hours with 200 μg/ml CII. The levels of IL-2, IL-4, IL-5, IL-10, IFNγ, and tumor necrosis factor α (TNFα) in the supernatants were measured by cytometric bead array (BD PharMingen), using the protocol provided by the manufacturer.

Histopathology. B6 or J_α281-knockout mice were killed and the fore paws removed 65 days after the induction of CIA or 10 days after K/BxN serum transfer. Paws were then fixed in buffered formalin, decalcified, embedded in paraffin, sectioned, and stained with hematoxylin and eosin.

RESULTS

Increase in liver NKT cells in CIA. To investigate the role of CD1-restricted V_α14 NKT cells in CIA, we first analyzed the number of V_α14 NKT cells using α-GC–loaded CD1 dimer. As shown in Figure 1A, the percentage of α-GC–loaded CD1-reactive V_α14 NKT cells among total liver mononuclear cells and peripheral blood mononuclear cells (PBMCs) was increased in CIA mice compared with control mice treated with CFA alone. The absolute number of α-GC–loaded CD1-reactive V_α14 NKT cells was also increased in the liver at the peak of the disease (Figure 1B).

Amelioration of CIA by anti-CD1 mAb treatment. To elucidate the role of V_α14 NKT cells in the pathogenesis of arthritis, we next examined the effect of anti-CD1d mAb on the development of CIA. We immunized DBA1/J mice and then administered intraperitoneal injections of either anti-CD1d mAb or control rat IgG twice per week starting from the day of the second immunization (5). As shown in Figure 2A, anti-CD1d treatment ameliorated arthritis in the mAb treatment

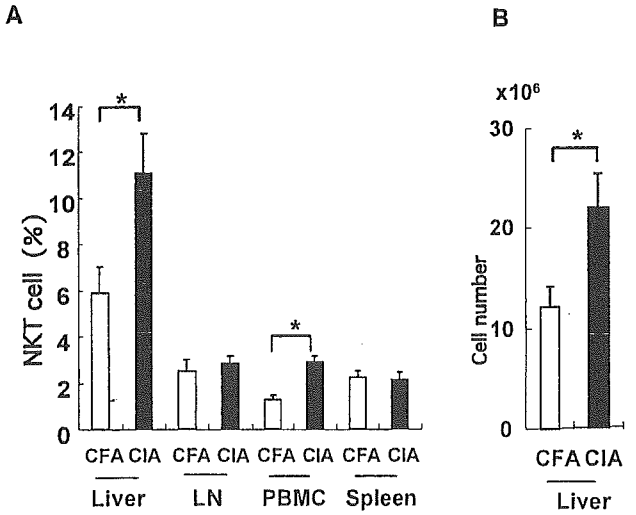

Figure 1. Expression of natural killer T (NKT) cells in the collagen-induced arthritis (CIA) model. **A,** To determine the frequency of NKT cells in various organs of mice with CIA or control mice (treated with Freund's complete adjuvant [CFA]), cells were obtained from the mice at the time of death, 30–35 days after the first immunization. Results are expressed as the percentage of α-galactosylceramide–loaded CD1d-positive T cells within the lymphocyte gates. LN = lymph nodes; PBMC = peripheral blood mononuclear cells. **B,** Absolute numbers of NKT cells in the liver were calculated from the total liver mononuclear cells of the same mice as in **A.** Bars show the mean and SEM of 7–8 mice per group. * = $P < 0.05$, by Mann-Whitney U test.

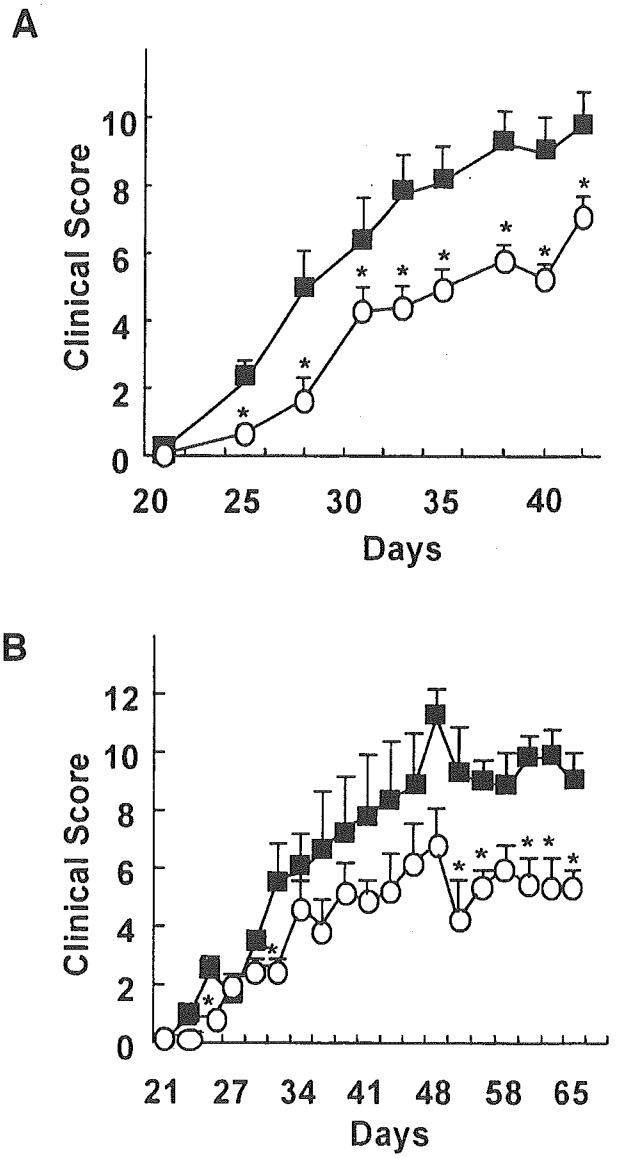

Figure 2. Amelioration of collagen-induced arthritis (CIA) in **A,** anti-CD1 monoclonal antibody (mAb)–treated or **B,** natural killer T cell–deficient mice. **A,** The clinical course of CIA was monitored in DBA/1 mice treated with 250 μg of anti-CD1d mAb (○) or control rat IgG (■), twice per week starting from day 21 after the first immunization. Bars show the mean and SEM of 13 mice (6-week-old males) per group from 2 independent experiments (n = 5 or 8 per group). * = $P < 0.05$ versus control IgG-treated mice, by Mann-Whitney U test. **B,** The clinical course of CIA was monitored in J_α281-knockout (○) and wild-type B6 (■) mice immunized with chicken type II collagen emulsified with Freund's complete adjuvant. Bars show the mean and SEM of 5 mice per group. * = $P < 0.05$ versus B6 mice, by Mann-Whitney U test.

group as compared with that in the control group. Disease susceptibility was not different between anti-CD1d–treated mice and control mice. This result suggests that CD1d-restricted $V_\alpha14$ NKT cells contribute to the enhancement of the disease course in CIA.

Reduced severity of CIA in NKT cell–deficient mice. To further investigate the contribution of CD1-restricted $V_\alpha14$ NKT cells to arthritis, we induced CIA in $V_\alpha14$ NKT cell–deficient $J_\alpha281$-knockout mice. As shown in Figure 2B, $V_\alpha14$ NKT cell–deficient mice developed less severe arthritis compared with that in the wild-type B6 mice. Disease susceptibility was not different between B6 mice and $J_\alpha281$-knockout mice. This result further supports the idea that $V_\alpha14$ NKT cells could play a role in the enhancement of CIA.

Altered CII-specific responses in NKT cell–deficient mice. To examine whether the response to CII was altered in the presence or absence of $V_\alpha14$ NKT cells, we measured CII-specific IgG isotype levels 65 days after the induction of CIA. It is generally accepted that elevation of autoantigen-specific IgG2a antibody is the result of augmentation of the Th1 immune response to the antigen, whereas a higher level of IgG1 antibody is a reflection of a stronger Th2 response to the antigen. In $J_\alpha281$-knockout mice, there was a slight reduction in the level of antigen-specific IgG2a antibody and an increase in the level of antigen-specific IgG1 compared with that in wild-type B6 mice (Figure 3A). Consequently, the IgG1:IgG2a ratio was elevated in $J_\alpha281$-knockout mice, suggesting that $V_\alpha14$ NKT cell deficiency alters the Th1/Th2 balance in response to CII.

To further analyze the CII-reactive T cell response, we isolated the draining lymph node cells from B6 or $J_\alpha281$-knockout mice 10 days after the second immunization with CII, and stimulated the lymphoid cells with CII in vitro. We then compared the concentrations of IL-2, IL-4, IL-5, IL-10, IFNγ, and TNFα in the culture supernatants. The level of IL-10 was significantly increased in the supernatant obtained from the culture of lymphoid cells of $J_\alpha281$-knockout mice compared with those from B6 mice (Figure 3B). The concentrations of IL-2 and IFNγ were decreased in $J_\alpha281$-knockout mice; however, the levels of these cytokines were also very low in B6 mice. The concentration of TNFα was not different between these mice. IL-4 and IL-5 were not detected in either culture supernatant. These results suggest that $V_\alpha14$ NKT cells contribute to the alteration of the Th1/Th2 balance of the T cell response to CII.

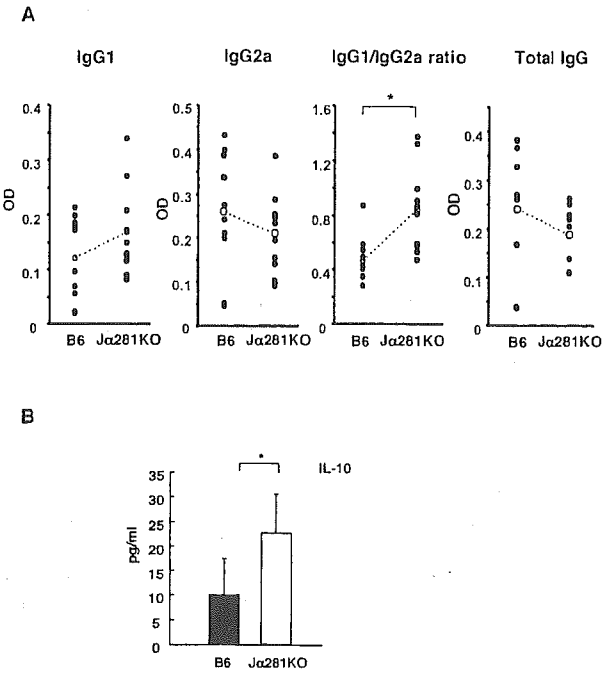

Figure 3. Altered type II collagen (CII)–specific responses in natural killer T cell–deficient mice. **A,** To determine the CII-specific antibody isotype levels in $J_\alpha281$-knockout (Jα281KO) mice as compared with wild-type B6 mice, individual serum samples obtained on day 65 after induction of arthritis were analyzed by enzyme-linked immunosorbent assay, with results expressed as the optical density (OD). Open circles with broken lines denote the average of individual samples. * = $P <$ 0.05, by Student's *t*-test. **B,** To determine the CII-specific T cell response in Jα281KO as compared with wild-type B6 mice, production of interleukin-10 (IL-10) (among other cytokines) from draining lymph node cells was analyzed by cytometric bead array. Bars show the mean and SEM of 3 mice per group. * = $P < 0.05$, by Mann-Whitney U test.

Amelioration of antibody-induced arthritis in NKT cell–deficient mice. CIA, commonly used as a model of RA, is characterized both by a primary immune response and by inflammation, and these features are often interdependent and therefore difficult to separate. In antibody-induced arthritis, inflammation occurs in the absence of a primary immune response, allowing us to investigate the effector mechanisms that link the potentially pathogenic antibodies and the overt development of arthritis (20). To address the role of $V_\alpha14$ NKT cells in the inflammatory process in addition to the modulation of the T cell response, we studied the role of $V_\alpha14$ NKT cells in anti-CII antibody–induced arthritis. To induce arthritis, mice received a mixture of 4 mAb reactive to CII, followed 72 hours later by LPS. As shown in Figure 4, compared with that in control animals, the severity of joint inflammation was signifi-

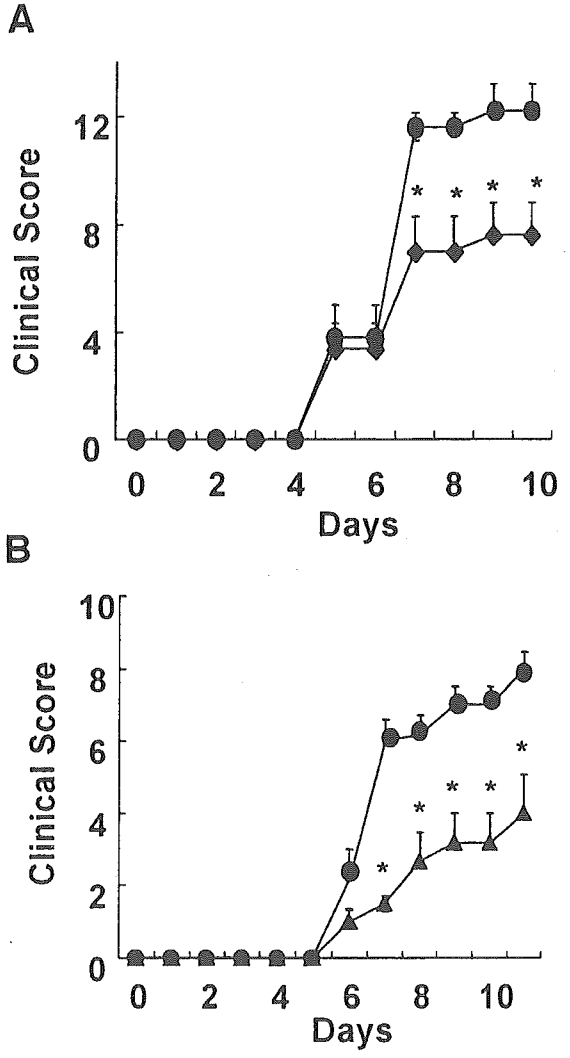

Figure 4. Reduced severity of anti–type II collagen monoclonal antibody (anti-CII mAb)–induced arthritis in natural killer T cell–deficient mice. The clinical course of arthritis induced by injection of a mixture of anti-CII mAb and lipopolysaccharide was monitored in 7-week-old female A, J_α281-knockout mice (◆) and B, CD1-knockout mice (▲) as compared with B6 mice (● in A and B). Bars show the mean and SEM of 5 mice per group, with representative data from 1 of 2 experiments. * = $P < 0.05$ versus B6 mice, by Mann-Whitney U test.

cantly reduced in J_α281-knockout mice as well as in CD1d-knockout mice, another NKT cell–deficient type of mouse (17). Disease susceptibility was not different among these 3 groups.

Arthritis induced by K/BxN serum transfer is another antibody-induced arthritis model (21). K/BxN is a recently developed model of inflammatory arthritis (18). K/BxN animals spontaneously develop arthritis

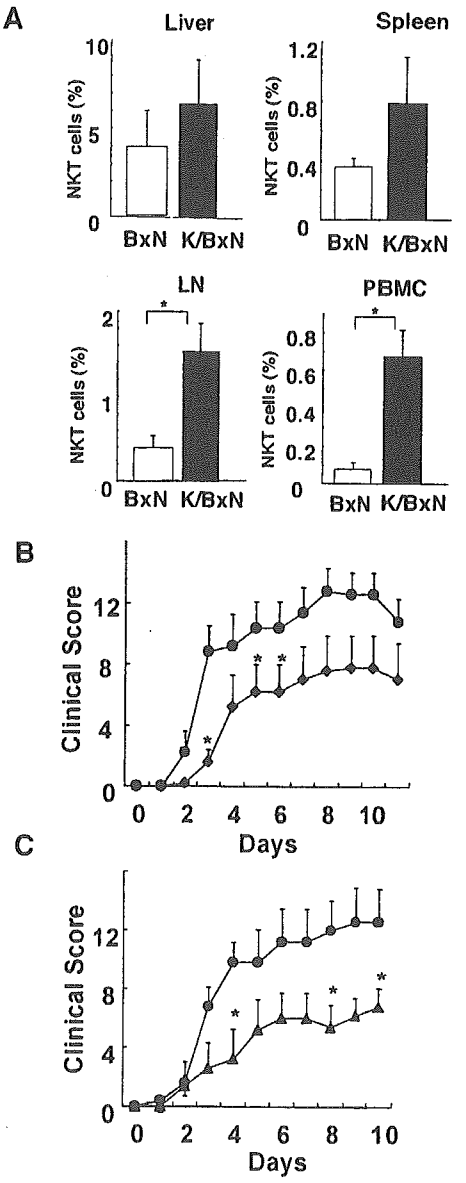

Figure 5. Reduced severity of arthritis induced by transfer of K/BxN serum in natural killer T (NKT) cell–deficient mice. A, To determine the frequency of NKT cells in various organs of mice with K/BxN serum–induced arthritis or BxN serum–transferred control mice, cells were obtained from the mice at the time of death, 10 days after serum transfer. Results are expressed as the percentage of α-galactosylceramide–loaded CD1-positive T cells within the lymphocyte gates. Bars show the mean and SEM of 3 mice per group. * = $P < 0.05$, by Mann-Whitney U test. LN = lymph nodes; PBMC = peripheral blood mononuclear cells. B and C, The clinical course of arthritis induced by the injection of K/BxN serum was monitored in 8-week-old female B, J_α281-knockout mice (◆) and C, CD1-knockout mice (▲) as compared with B6 mice (● in B and C). Bars show the mean and SEM of 5 mice per group, with representative data from 1 of 2 experiments. * = $P < 0.05$, by Mann-Whitney U test.

Figure 6. Histopathologic assessment of arthritic wrist joints. The joints from B6 mice and J_α281-knockout mice with collagen-induced arthritis (**A** and **B**, respectively) and from B6 mice and J_α281-knockout mice with K/BxN serum–transferred arthritis (**C** and **D**, respectively) were assessed for the extent of arthritis. Two mice per group were analyzed, and representative results are shown. (Hematoxylin and eosin stained; original magnification × 20.)

that is similar to RA in humans. The arthritis is initiated by T and B cell autoreactivity to a ubiquitously expressed antigen, glucose-6-phosphate-isomerase (GPI) (22). Transfer of serum from arthritic K/BxN mice into healthy animals provokes arthritis within days, independent of the response of T and B cells. K/BxN serum–induced arthritis is mediated by anti-GPI IgG.

With this arthritis model, we analyzed the number of V_α14 NKT cells, utilizing α-GC–loaded CD1 dimer. As shown in Figure 5A, the percentage of α-GC–loaded CD1-restricted V_α14 NKT cells among lymph node cells and PBMCs in arthritic mice was increased compared with that in control mice transferred with BxN serum. CD1-restricted V_α14 NKT cells among total liver mononuclear cells and splenocytes tended to be increased in arthritic mice. As shown in Figures 5B and C, the severity of joint inflammation was significantly reduced in J_α281-knockout mice and CD1d-knockout mice, respectively, as compared with that in control animals, which is consistent with the results observed in anti-CII antibody–induced arthritis. Disease susceptibility was not different among these 3 groups. These results indicate that V_α14 NKT cells contribute to the inflammatory effector phase of arthritis.

Histopathologic assessment of arthritis in J_α281-knockout mice. In addition to visual scoring of disease severity, we analyzed the histologic features in the joints of the fore paws of J_α281-knockout mice and wild-type B6 mice on day 65 after CIA induction or 10 days after K/BxN serum transfer. As shown in Figure 6A, following arthritis development in B6 mice, there was severe disease in the joints, associated with massive cell infiltration, cartilage erosion, and bone destruction. These histologic features were significantly less apparent in J_α281-knockout mice (Figure 6B). In K/BxN serum–transferred B6 mice, massive cell infiltration as well as

cartilage erosion and bone destruction were observed (Figure 6C). Infiltration of inflammatory cells was less evident and destruction of cartilage and bone were not apparent in J_α281-knockout mice (Figure 6D). These results support the idea that loss of V_α14 NKT cells ameliorates arthritis.

DISCUSSION

In this study, we demonstrated that blocking the interaction of CD1d and V_α14 NKT cells leads to the amelioration of CIA. We also showed that the severity of the disease induced in V_α14 NKT cell–deficient J_α281-knockout mice was reduced compared with that in wild-type B6 mice. In J_α281-knockout mice, the ratio of IgG1:IgG2a anti-CII antibody was elevated and production of IL-10 upon stimulation with CII was increased, suggesting that the response to CII was deviated to the Th2 response in these mice. Furthermore, we found that the disease was less severe in J_α281- and CD1-knockout mice with antibody-induced arthritis.

The most extensively used animal model of RA is CIA, which is accompanied by a predominant Th1 response and is characterized by production of the proinflammatory cytokines IFNγ and TNFα. Previous studies have shown that treatment with Th2-promoting cytokines or with mAb directed against Th1-promoting cytokines can effectively protect mice against CIA (23). V_α14 NKT cells were previously reported to protect other Th1 cell–mediated autoimmune diseases such as type I diabetes in NOD mice, by inducing a shift toward a Th2 T cell response to autoantigens (6–8). The development of diabetes was prevented either by infusion of NKT cell–enriched thymocyte preparations or by an increase of NKT cells in V_α14–J_α281–transgenic NOD mice (24,25). In contrast, V_α14 NKT cells appeared to exacerbate arthritis in the present study, since the severity of the disease was decreased in J_α281-knockout mice and anti-CD1d mAb treatment ameliorated the disease.

Because V_α14 NKT cells produce large amounts of both IL-4 and IFNγ upon stimulation with anti-CD3 antibody or its prototypic ligand α-GC, a regulatory role in Th cell differentiation has been proposed for these cells. However, the results obtained from α-GC treatment of B6 mice on Th cell differentiation are conflicting. The administration of α-GC was found to facilitate either Th1 differentiation or Th2 differentiation (26,27). Although the basis for these inconsistencies is not clear, the discrepancies between these results could be due to the differences in the protocols of the α-GC treatment, suggesting that small differences in circumstances may affect the immunomodulatory effect of V_α14 NKT cells. Recently, microbial products or proinflammatory cytokines such as IL-12 have been reported to amplify the basal weak responses of CD1d-restricted T cells to self antigens to yield potent effector functions by enhancing IFNγ secretion (28). Abundant proinflammatory cytokines may modulate the function of V_α14 NKT cells in mice with CIA.

Recent studies using the serum of an engineered mouse model, K/BxN, have revealed that autoantibodies, complement components, Fc receptors, and cytokines such as IL-1 and TNFα participate in the pathogenesis of antibody-mediated erosive arthritis (29–31). As cellular components, neutrophils and mast cells have been reported to be essential for antibody-mediated inflammatory arthritis (32,33). We showed, in this study, that mice deficient in V_α14 NKT cells exhibited a reduced severity of antibody-mediated arthritis, suggesting that V_α14 NKT cells act as effector cells in inflammatory arthritis. Potential V_α14 NKT cell effector mechanisms that may be important for the induction and progression of joint inflammation include the rapid production of a variety of cytokines, including IL-1 and TNFα, that play a critical role in both K/BxN serum–induced arthritis and anti-CII mAb–induced arthritis, as well as in human RA (1,30,31,34). Very recently, Kim et al reported that NKT cells promote K/BxN serum–induced joint inflammation by producing IL-4 and IFNγ (35). Those authors showed that IL-4 and IFNγ are important in reducing the production of transforming growth factor β (TGFβ), resulting in suppression of arthritis. The regulation of TGFβ by NKT cells might be one of the important mechanisms controlling the inhibition of arthritis.

In this study we have demonstrated that V_α14 NKT cells could contribute to the pathogenesis of arthritis in several ways, including enhancing the inflammatory effector phase of arthritis mediated by autoantibodies. Changing the Th1/Th2 balance of autoantigen-reactive T cells by V_α14 NKT cells may also contribute to the pathogenesis of CIA. As we previously proposed, modulation of the function of V_α14 NKT cells with proper stimuli, such as the Th2-skewing glycolipid ligand, OCH, or a blocking reagent for NKT cell functions, could be considered as new therapeutic interventions in the management of RA.

ACKNOWLEDGMENTS

We thank Masaru Taniguchi at the Riken Research Center for Allergy and Immunology for providing the J_α281-

knockout mice, Steven Balk at Beth Israel Deaconess Medical Center and Harvard Medical School for providing the CD1-knockout mice, and Drs. Christophe Benoist and Diane Mathis, Joslin Diabetes Center and Harvard Medical School and Institu de Genetique et de Biologie Moleculaire et Cellulaire for providing the TCR-transgenic mice. We also thank Miho Mizuno and Chiharu Tomi for excellent technical assistance. We are grateful to John Ludvic Croxford for critical reading of the manuscript.

REFERENCES

1. Feldmann M, Brennan FM, Maini RN. Role of cytokines in rheumatoid arthritis. Annu Rev Immunol 1996;14:397–440.
2. Brenner MB, Brigl M. CD1: antigen presentation and T cell function. Annu Rev Immunol 2004;22:817–90.
3. Taniguchi M, Harada M, Kojo S, Nakayama T, Wakao H. The regulatory role of Vα14 NKT cells in innate and acquired immune response. Annu Rev Immunol 2003;21:483–513.
4. Kronenberg M, Gapin L. The unconventional lifestyle of NKT cells. Nat Rev Immunol 2002;2:557–68.
5. Chiba A, Oki S, Miyamoto K, Hashimoto H, Yamamura T, Miyake S. Suppression of collagen-induced arthritis by natural killer T cell activation with OCH, a sphingosine-truncated analog of α-galactosylceramide. Arthritis Rheum 2004;50:305–13.
6. Hammond KJ, Godrey DI. NKT cells: potential targets for autoimmune disease therapy? Tissue Antigens 2002;59:353–63.
7. Wilson SB, Delovitch TL. Janus-like role of regulatory iNKT cells in autoimmune disease and tumour immunity. Nat Rev Immunol 2003;3:211–22.
8. Hammond KJ, Kronenberg M. Natural killer T cells: natural or natural regulators of autoimmunity? Curr Opin Immunol 2003;15: 683–9.
9. Sumida T, Sakamoto A, Murata H, Makino Y, Takahashi H, Yoshida S, et al. Selective reduction of T cells bearing invariant Vα24JαQ antigen receptor in patients with systemic sclerosis. J Exp Med 1995;182:1163–8.
10. Wilson SB, Kent SC, Patton KT, Orban T, Jackson RA, Exley M, et al. Extreme Th1 bias of invariant Vα24JαQ T cells in type 1 diabetes. Nature 1998;391:177–81.
11. Illes Z, Kondo T, Newcombe J, Oka N, Tabira T, Yamamura T. Differential expression of NK T cell Vα24JαQ invariant TCR chain in the lesions of multiple sclerosis and chronic inflammatory demyelinating polyneuropathy. J Immunol 2000;164:4375–81.
12. Kojo S, Adachi Y, Keino H, Taniguchi M, Sumida T. Dysfunction of T cell receptor AV24AJ18+, BV11+ double-negative regulatory natural killer T cells in autoimmune diseases. Arthritis Rheum 2001;44:1127–38.
13. Yoshimoto T, Bendelac A, Hu-Li J, Paul WE. Defective IgE production by SJL mice is linked to the absence of CD4+, NK1.1+ T cells that promptly produce interleukin 4. Proc Natl Acad Sci U S A 1995;92:11931–4.
14. Mieza MA, Itoh T, Cui JQ, Makino Y, Kawano T, Tsuchida K, et al. Selective reduction of Vα14+ NK T cells associated with disease development in autoimmune-prone mice. J Immunol 1996;156:4035–40.
15. Gombert JM, Herbelin A, Tancrede-Bohin E, Dy M, Carnaud C, Bach JF. Early quantitative and functional deficiency of $NK1^+$-like thymocytes in the NOD mouse. Eur J Immunol 1996;26:2989–98.
16. Cui J, Shin T, Kawano T, Sato H, Kondo E, Toura I, et al. Requirement for Vα14 NKT cells in IL-12-mediated rejection of tumors. Science 1997;278:1623–6.
17. Sonoda KH, Exley M, Snapper S, Balk SP, Stein-Streilein J. CD1-reactive natural killer T cells are required for development of systemic tolerance through an immune-privileged site. J Exp Me 2003;3:211–22.
18. Kouskoff V, Korganow AS, Duchatelle V, Degott C, Benoist Mathis D. Organ-specific disease provoked by systemic autoimm nity. Cell 1996;87:811–22.
19. Szalay G, Ladel CH, Blum C, Brossay L, Kronenberg M, Kau mann SH. Anti-CD1 monoclonal antibody treatment reverses tl production patterns of TGF-β2 and Th1 cytokines and ameliorat listerosis in mice. J Immunol 1999;162:6955–8.
20. Terato K, Hasty KA, Reife RA, Cremer MA, Kang H, Stuart JN Induction of arthritis with monoclonal antibodies to collage J Immunol 1992;148:2103–8.
21. Korganow AS, Ji H, Mangialaio S, Dchatelle V, Pelanda R, Mart T, et al. From systemic T cell self-reactivity to organ-specif autoimmune disease via immunoglobulins. Immunity 1999;1 451–61.
22. Matsumoto I, Staub A, Benoist C, Mathis D. Arthritis provoked l linked T and B cell recognition of a glycolytic enzyme. Scien 1999;286:1732–5.
23. Van Roon JA, Lafeber FP, Bijlsma JW. Synergistic activity interleukin-4 and interleukin-10 in suppression of inflammatic and joint destruction in rheumatoid arthritis [review]. Arthri Rheum 2001;44:3–12.
24. Hammond KJ, Poulton LD, Palmisano LJ, Silveria PA, Godfr DJ, Baxter AG. α/β-T cell receptor+CD4−CD8−(NKT) thym cytes prevent insulin-dependent diabetes mellitus in nonobe diabetic (NOD)/Lt mice by the influence of interleukin (IL) and/or IL-10. J Exp Med 1998;187:1047–56.
25. Lehuen A, Lantz O, Beaudoin L, Laloux V, Carnaud C, Bendel A, et al. Overexpression of natural killer T cells protects Vα1 Jα281 transgenic nonobese diabetic mice against diabetes. J E: Med 1998;188:1831–9.
26. Singh N, Hong S, Scherer DC, Serizawa I, Burdin N, Kronenbe M, et al. Activation of NKT cells by CD1d and α-galactosylcera ide directs conventional T cells to the acquisition of a Tl phenotype. J Immunol 1999;163:2373–7.
27. Cui J, Watanabe N, Kawano T, Yamashita M, Kamata T, Shimi C, et al. Inhibition of T helper cell type 2 cell differentiation a immunoglobulin E response by ligand-activated Vα14 natu killer T cells. J Exp Med 1999;190:783–92.
28. Brigl M, Bry L, Kent SC, Gumperz JE, Brenner MB. Mechanis of CD1d-restricted natural killer T cell activation during microbi infection. Nat Immunol 2003;12:1230–7.
29. Ji H, Ohmura K, Mahmood U, Lee DM, Hofhuis FM, Boackle S. et al. Arthritis critically dependent on innate immune syste players. Immunity 2002;16:157–68.
30. Kagari T, Doi H, Shimozato T. The importance of IL-1β a TNF-α, and the noninvolvement of IL-6, in the development monoclonal antibody-induced arthritis. J Immunol 2002;1€ 1459–66.
31. Ji H, Pettit A, Ohmura K, Ortiz-Lopez A, Duchatelle V, Degott et al. Critical roles for interleukin 1 and tumor necrosis factor α antibody-induced arthritis. J Exp Med 2002;196:77–85.
32. Wipke BT, Allen PM. Essential role of neutrophils in the initiati and progression of a murine model of rheumatoid arthrit J Immunol 2001;167:1601–8.
33. Lee DM, Friend DS, Gurish MF, Benoist C, Mathis D, Brenn MB. Mast cells: a cellular link between autoantibodies and infla matory arthritis. Science 2002;297:1689–92.
34. Oki S, Chiba A, Yamamura T, Miyake S. The clinical implicati and molecular mechanism of preferential IL-4 production modified glycolipid-stimulated NKT cells. J Clin Invest 2004;11 1631–40.
35. Kim HY, Kim HJ, Min HS, Kim S, Park WS, Park SH, et al. NK cells promote antibody-induced joint inflammation by suppressi transforming growth factor β1 production. J Exp Med 2005;2(41–7.

Available online at www.sciencedirect.com
SCIENCE DIRECT®
Tetrahedron Letters
ELSEVIER
Tetrahedron Letters 46 (2005) 5043–5047

A concise synthesis of (3*S*,4*S*,5*R*)-1-(α-D-galactopyranosyl)-3-tetracosanoylamino-4,5-decanediol, a *C*-glycoside analogue of immunomodulating α-galactosylceramide OCH

Tetsuya Toba,[a] Kenji Murata,[a] Takashi Yamamura,[b] Sachiko Miyake[b] and Hirokazu Annoura[a,*]

[a]*Biomedical Research Laboratories, Daiichi Suntory Pharma Co., Ltd., 1-1-1, Wakayamadai, Shimamoto-cho, Mishima-gun, Osaka 618-8513, Japan*
[b]*Department of Immunology, National Institute of Neuroscience, NCNP, Tokyo 187-8502, Japan*

Received 1 February 2005; revised 13 May 2005; accepted 18 May 2005
Available online 9 June 2005

Abstract—A concise and convergent synthesis of the *C*-glycoside analogue **2b** of immunomodulating α-galactosylceramide OCH **1b** starting from readily available 2,3,4,6-tetra-*O*-benzyl-D-galactose **3** and L-arabinose **6** is described. The synthesis features the nucleophilic addition of an α-ethynyl sugar **5** to the phytosphingosine-precursor aldehyde **9** and would be applicable to a variety of *C*-glycoside analogues of interest.

Natural killer (NK) T cells are potent producers of immunoregulatory cytokines and specific for glycolipid antigens bound by a nonclassical major histocompatibility complex (MHC) class I-like molecule, CD1d.[1] The glycolipids, an α-galactosylceramide named KRN7000 **1a**[2] and an altered analogue termed OCH **1b** possessing a shorter C5 sphingosine side chain,[3] have been identified as NKT cell ligands (Fig. 1). Compound **1b** was shown to induce a predominant production of interleukin (IL)-4, a key Th2 cytokine engaged in autoimmunity control, over Th1 cytokine interferon (IFN)-γ, while **1a** induced both Th1/Th2 cytokines. Only compound **1b** but not **1a** is significantly effective in animal models of Th1-mediated autoimmune diseases such as experimental autoimmune encephalomyelitis (EAE) and collagen induced arthritis (CIA).[3,4] Quite recently, we have reported a practical and efficient synthesis of **1b** in 12 steps and 19% overall yield from commercially available D-arabitol.[5] It is often a conventional strategy to synthesize the *C*-glycoside analogue of biologically active *O*-glycosides, since *C*-glycosides are in general resistant to enzymatic degradation by glycosidases and may exhibit longer duration of action. It has recently been demonstrated that conversion of **1a** to its *C*-glycoside analogue **2a** leads to striking enhancement of activity on in vivo animal models of malaria and lung cancer

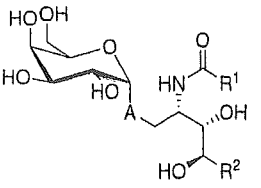

1a (KRN7000; A = O, $R^1 = n\text{-}C_{25}H_{51}$, $R^2 = n\text{-}C_{14}H_{29}$)
1b (OCH; A = O, $R^1 = n\text{-}C_{23}H_{47}$, $R^2 = n\text{-}C_5H_{11}$)
2a (A = CH_2, $R^1 = n\text{-}C_{25}H_{51}$, $R^2 = n\text{-}C_{14}H_{29}$)
2b (A = CH_2, $R^1 = n\text{-}C_{23}H_{47}$, $R^2 = n\text{-}C_5H_{11}$)

Figure 1. Structure of α-galactosylceramides **1a,b** and their *C*-glycoside analogues **2a,b**.

Keywords: *C*-glycoside; OCH; Ceramide; CD1d; NKT cell ligand.
Abbreviations: TMSOTf, trimethylsilyl trifluoromethanesulfonate; PTSA, *p*-toluenesufonic acid; MTPA, 2-methoxy-2-phenyl-2-(trifluoromethyl)acetic acid; DME, 1,2-dimethoxyethane; EDCI·HCl, 1-[3-(dimethylamino)propyl]-3-ethylcarbodiimide hydrochloride; HOAt, 1-hydroxy-7-azabenzotriazole.
* Corresponding author. Tel.: +81 75 962 8188; fax: +81 75 962 6448; e-mail: hirokazu_annoura@dsup.co.jp

0040-4039/$ - see front matter © 2005 Elsevier Ltd. All rights reserved.
doi:10.1016/j.tetlet.2005.05.069

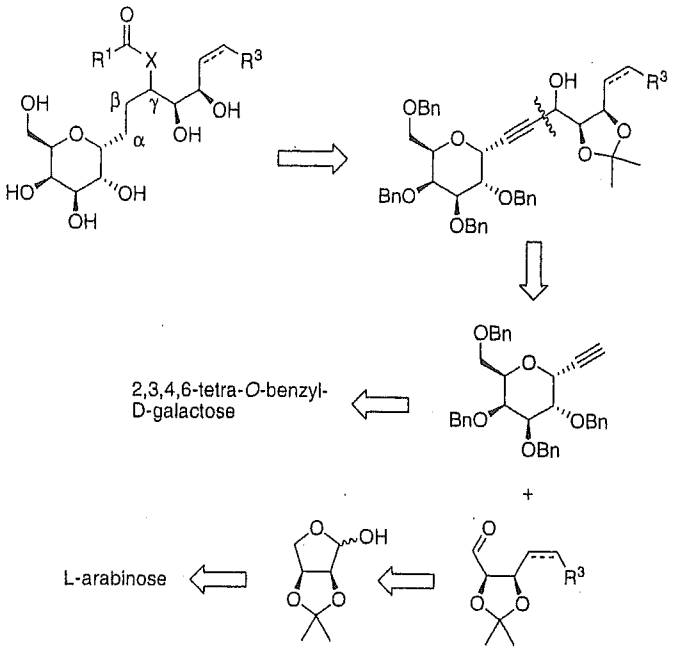

Figure 2. Retrosynthetic analysis of *C*-glycolipids.

by inducing prolonged production of the Th1 cytokines IFN-γ and IL-12.[6]

These results prompted us to investigate a short and versatile synthetic pathway applicable to the *C*-glycoside analogues of **1b** and related compounds. There have been only a few reports on the synthesis of **2a** to date, that utilize Wittig reaction,[7] Ramberg–Bäcklund reaction followed by β-selective hydrogenation from the diisopropylsilyl protecting group,[6b] or olefin cross-metathesis for the installation of the *C*-glycoside linkage.[8] We present herein a concise and short synthesis of **2b**, which is independent of previous methodologies for **2a** and would be applicable to a variety of phytosphingosine derivatives in terms of chain length and substitution, including aromatic groups and heteroatoms.

Our retrosynthetic analysis for **2b** revealed a straightforward and versatile strategy based on the nucleophilic addition of an α-ethynyl sugar to the phytosphingosine-precursor aldehyde synthesized from L-arabinose (Fig. 2). The critical feature of our strategy is the dissecting position, which former retrosyntheses of **2a** all cleaved between the α- and β-carbons of the anomeric center, while we chose between the β-and γ-carbons. This allowed the shorter and expansive synthesis at the expense of a need to construct a new stereocenter.

Perbenzylated 1-deoxy-1-α-ethynyl-galactopyranose **5** was prepared from commercially available 2,3,4,6-tetra-*O*-benzyl-D-galactose **3** in three steps (Scheme 1).[9] Thus, compound **3** was quantitatively acetylated and α-face selectively coupled with tri-*n*-butyl(trimethylsilylethynyl)tin in the presence of TMSOTf and MS-4A to give **4** ($^3J_{anomericHH}$ = 5.7 Hz) in 60% yield. The corresponding β-isomer of **4** was not detected but a small amount of **3**, presumably due to hydrolysis of the acetylated

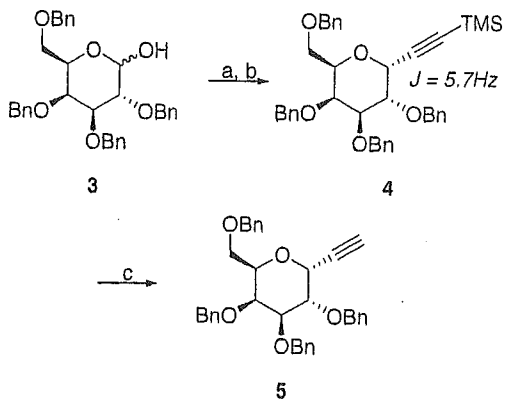

Scheme 1. Reagents and conditions: (a) Ac_2O, pyridine, CH_2Cl_2, 0 °C to rt (quant.); (b) tri-*n*-butyl(trimethylsilylethynyl)tin, TMSOTf, MS4A, CH_2Cl_2, rt (60%); (c) 1 N NaOH, MeOH, CH_2Cl_2, rt (quant.).

substrate, was detected by TLC. Desilylation of **4** was accomplished by NaOH–MeOH to give the desired compound **5** quantitatively.

The counterpart **9** was efficiently synthesized from L-arabinose **6** endowed with suitable stereochemistry corresponding to the vicinal hydroxyl groups in the phytosphingosine moiety (Scheme 2). Thus, compound **6** was protected as a 3,4-*O*-acetonide, reduced to a triol and subjected to $NaIO_4$ degradation to produce 2,3-*O*-isopropylidene-L-erythrose **7**[10] in 71% overall yield. Four carbon homologation by Wittig reaction followed by hydrogenation and standard Swern oxidation of the primary alcohol produced the requisite aldehyde **9** in 61% overall yield. No epimerization of **9** was observed neither during the reaction nor after storing overnight at −20 °C.

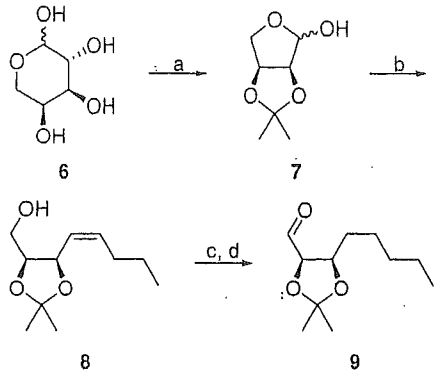

Scheme 2. Reagents and conditions: (a) (i) $Me_2C(OMe)_2$, PTSA, DMF, rt, (ii) $NaBH_4$, EtOH, rt, (iii) $NaIO_4$, H_2O, rt (71%; three steps); (b) *n*-$BuPh_3PBr$, *n*-BuLi, THF, −78 °C to rt (79%); (c) H_2, Pd/C, EtOH, rt (96%); (d) DMSO, $(COCl)_2$, CH_2Cl_2, −78 to 0 °C (80%).

Next, the coupling reaction of **5** and **9** was examined using various metal acetylide ions. This key step requires the generation of an adequate stereochemistry at the epimeric propargylic hydroxyl group. When the lithium acetylide derived from **5** was employed, the reaction gave a 3.2:2 mixture of diastereomers, **10a** and **10b**, in 47% and 30% yields, respectively, on the basis of the recovered starting materials[11] (Scheme 3). Compounds **10a** and **10b** were easily separated by column chromatography over silica gel using *n*-hexane/EtOAc (10:1). The stereochemistry of the propargylic hydroxyl group was determined for the more polar isomer **10a** to be the *R*-isomer by applying modified Mosher's protocol (Fig. 3).[12,13] Other attempts of chelation-controlled addition reaction utilizing Zn or Mg species[14] did not improve the diastereoselectivity and decreased the chemical yields.[15]

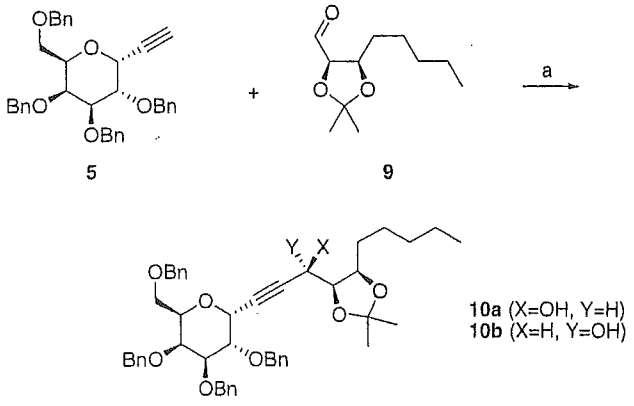

Scheme 3. Reagents and conditions: (a) *n*-BuLi, THF, −48 to −30 °C (47% yield for **10a**, 30% yield for **10b**).

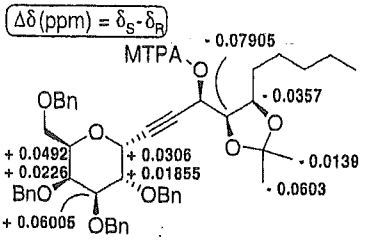

Figure 3. $\Delta\delta$ values for the MTPA esters of **10a**.

Once the key intermediate **10a** was available, the synthesis of **2b** was completed in a straightforward and efficient manner (Scheme 4). Thus, reduction of the triple bond in **10a** with $TsNHNH_2$ followed by mesylation of the hydroxyl group gave **11** in 86% yield. Compound **11** was azidated, reduced to an amine by hydrogenation and consecutively acylated with *n*-tetracosanoic acid to afford amide **12** in 48% overall yield. Finally, deprotection of the isopropylidene acetal of **12** under acidic conditions and subsequent removal of the benzyl groups by hydrogenation furnished **2b** in 88% yield. The synthetic sample displayed satisfactory ^1H NMR spectrum and was confirmed by high-resolution mass spectrum

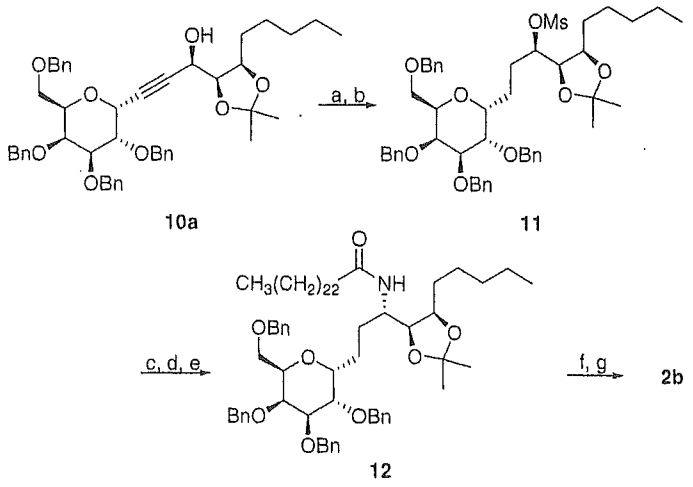

Scheme 4. Reagents and conditions: (a) $TsNHNH_2$, DME, NaOAc aq, reflux (91%); (b) MsCl, Pyridine, CH_2Cl_2, 0 °C to rt (94%); (c) NaN_3, DMF, 90 °C; (d) H_2, $Pd/CaCO_3$, EtOH, rt; (e) tetracosanoic acid, EDCI·HCl, HOAt, Et_3N, DMF–CH_2Cl_2, rt (48%; three steps); (f) 80% AcOH, 60 °C (88%); (g) H_2, $Pd(OH)_2/C$, MeOH–CH_2Cl_2, rt (quant.).

(HR-MS).[16] Compound **2b** did not show in vitro IL-4 and IFN-γ production in splenocytes but increased serum level of IL-4 in C57BL/6 mice in vivo. Thus, compound **2b** proved to possess the pharmacological profiles distinctively different from that of **1b** from the preliminary results of biological testing.[17] Similar pharmacological differences have been reported between **1a** and its *C*-glycolipid **2a**,[6] which support our findings.

In conclusion, we have developed a concise protocol for the synthesis of **2b** involving only 12 steps starting from commercially available 2,3,4,6-tetra-*O*-benzyl-D-galactose **3** and L-arabinose **6**. Although the coupling reaction of **5** and **9** proceeded but not yet with sufficient stereoselectivity, the total sequence of this method is more convergent and versatile compared with those previously reported for **2a**,[6b,7,8] since the two obtained diastereomers **10a** and **10b** can be easily separated by conventional purification procedures. Consequently, this new synthetic route would enable the synthesis of a variety of *C*-glycoside analogues of phytosphingolipids related to **1a** and **1b**, especially those which vary in the sphingosine side chain length or substituents other than aliphatic alkyl groups. In addition, it should be noted that this route promises to contribute significantly for clarifying the structure–activity relationships (SARs) of this series of *C*-glycosides of interest. The SAR study in this series of compounds will be reported in due course.

Acknowledgements

We thank Ms. K. Nakanishi for her initial contribution to this synthetic work. We also thank Drs. M. Masumura, Y. Tanaka, and Ms. M. Goto for carrying out biological testing. Drs. T. Nishihara and G. Nakayama are acknowledged for their supports and encouragement throughout this study.

References and notes

1. For reviews: (a) Porcelli, S. A.; Modlin, R. L. *Annu. Rev. Immunol.* **1999**, *17*, 297–329; (b) Hong, S.; Scherer, D. C.; Singh, N.; Mendiratta, S. K.; Serizawa, I.; Koezuka, Y.; Van Kaer, L. *Immunol. Rev.* **1999**, *169*, 31–44; (c) Sidobre, S.; Kronenberg, M. *J. Immunol. Methods* **2002**, *268*, 107–121; (d) Wilson, M. T.; Van Kaer, L. *Curr. Pharm. Des.* **2003**, *9*, 201–220; (e) Cox, T. *Phil. Trans. R. Soc. Lond. B* **2003**, *358*, 967–973; (f) Brigl, M.; Brenner, M. B. *Annu. Rev. Immunol.* **2004**, *22*, 817–890.
2. (a) Morita, M.; Motoki, K.; Akimoto, K.; Natori, T.; Sakai, T.; Sawa, E.; Yamaji, K.; Koezuka, Y.; Kobayashi, E.; Fukushima, H. *J. Med. Chem.* **1995**, *38*, 2176–2187; (b) Morita, M.; Sawa, E.; Yamaji, K.; Sakai, T.; Natori, T.; Koezuka, Y.; Fukushima, H.; Akimoto, K. *Biosci. Biotechnol. Biochem.* **1996**, *60*, 288–292; (c) Takikawa, H.; Muto, S.; Mori, K. *Tetrahedron* **1998**, *54*, 3141–3150; (d) Graziani, A.; Passacantilli, P.; Piancatelli, G.; Tani, S. *Tetrahedron: Asymmetry* **2000**, *11*, 3921–3937.
3. (a) Miyamoto, K.; Miyake, S.; Yamamura, T. *Nature* **2001**, *413*, 531–534; (b) Yamamura, T.; Miyake, S. PCT Int. Appl. WO 2003/016326, 2003; *Chem. Abstr.* **2003**, *138*, 205292m; (c) Yamamura, T.; Miyamoto, K.; Illes, Z.; Pal, E.; Araki, M.; Miyake, S. *Curr. Top. Med. Chem.* **2004**, *4*, 561–567; (d) Oki, S.; Chiba, A.; Yamamura, T.; Miyake, S. *J. Clin. Invest.* **2004**, *113*, 1631–1640.
4. Chiba, A.; Oki, S.; Miyamoto, K.; Hashimoto, H.; Yamamura, T.; Miyake, S. *Arthritis Rheum.* **2004**, *50*, 305–313.
5. Murata, K.; Toba, T.; Nakanishi, K.; Takahashi, B.; Yamamura, T.; Miyake, S.; Annoura, H. *J. Org. Chem.* **2005**, *70*, 2398–2401.
6. (a) Schmieg, J.; Yang, G.; Frank, R. W.; Tsuji, M. *J. Exp. Med.* **2003**, *198*, 1631–1641; (b) Yang, G.; Schmieg, J.; Tsuji, M.; Frank, R. W. *Angew. Chem., Int. Ed.* **2004**, *43*, 3818–3822. This route consists of over 20 steps for the synthesis of **2a** upon counting on all the substep sequence.
7. Tomiyama, H.; Yanagisawa, T.; Nimura, M.; Noda, A.; Tomiyama, T. JP 2001/354666, 2002; *Chem. Abstr.* **2002**, *136*, 37901x. This route was unreproducible and the final product was unable to be isolated due to considerable amounts of inseparable contaminants.
8. Chen, G.; Schmieg, J.; Tsuji, M.; Franck, R. W. *Org. Lett.* **2004**, *6*, 4077–4080. This route has been improved compared with that reported in Ref. 6b and more practical for **2a** which completes in only 11 steps, however, it requires the commercially available phytosphingosine and is not expandable enough for analogue syntheses including **2b**. Preparing commercially unavailable phytosphingosine derivatives for this route must require several additional steps, which makes this route less attractive for SAR purposes; For examples of the syntheses of phytosphingosine derivatives, see: Lin, C.-C.; Fan, G.-T.; Fang, J.-M. *Tetrahedron Lett.* **2003**, *44*, 5281–5283; Chiu, H.-Y.; Tzou, D.-L. M.; Patkar, L. N.; Lin, C.-C. *J. Org. Chem.* **2003**, *68*, 5788–5791, and references cited therein.
9. Dondoni, A.; Mariotti, G.; Marra, A. *J. Org. Chem.* **2002**, *67*, 4475–4486.
10. Sabino, A. A.; Pilli, R. A. *Tetrahedron Lett.* **2002**, *43*, 2819–2821.
11. In this reaction, the starting α-ethynyl-galactopyranose **5** was usually recovered unchanged in over 15% yield.
12. Ohtani, I.; Kusumi, T.; Kashman, Y.; Kakisawa, H. *J. Am. Chem. Soc.* **1991**, *113*, 4092–4096.
13. ^{1}H NMR of (*S*)-MTPA ester of **10a** (400 MHz, $CDCl_3$): δ 7.6–7.55 (m, 2H), 7.4–7.2 (m, 23H), 5.65 (dd, 1H, *J* = 7.8 Hz, 1.7 Hz), 4.90 (d, 1H, *J* = 11.4 Hz), 4.83 (dd, 1H, *J* = 5.8 Hz, 1.7 Hz), 4.77 (d, 1H, *J* = 11.7 Hz), 4.73 (d, 1H, *J* = 11.8 Hz), 4.69 (d, 1H, *J* = 11.7 Hz), 4.64 (d, 1H, *J* = 11.8 Hz), 4.54 (d, 1H, *J* = 11.4 Hz), 4.44 (d, 1H, *J* = 11.9 Hz), 4.37 (d, 1H, *J* = 11.9 Hz), 4.18 (dd, 1H, *J* = 7.6 Hz, 5.8 Hz), 4.08 (dd, 1H, *J* = 9.7 Hz, 5.7 Hz), 4.15–4.05 (m, 1H), 4.01 (t, 3H, *J* = 6.2 Hz), 3.95–3.93 (m, 1H), 3.78 (dd, 1H, *J* = 9.8 Hz, 2.7 Hz), 3.49 (s, 3H), 3.5–3.4 (m, 2H), 1.6–1.5 (m, 2H), 1.55–1.4 (m, 1H), 1.39 (s, 3H), 1.27 (s, 3H), 1.3–1.1 (m, 5H), 0.82 (t, 3H, *J* = 6.5 Hz); ^{1}H NMR of (*R*)-MTPA ester of **10a** (400 MHz, $CDCl_3$): δ 7.6–7.57 (m, 2H), 7.5–7.2 (m, 23H), 5.66 (dd, 1H, *J* = 8.9 Hz, 1.8 Hz), 4.90 (d, 1H, *J* = 11.4 Hz), 4.80 (dd, 1H, *J* = 6.0 Hz, 1.8 Hz), 4.77 (d, 1H, *J* = 11.7 Hz), 4.69 (d, 1H, *J* = 11.7 Hz), 4.68 (d, 1H, *J* = 11.7 Hz), 4.61 (d, 1H, *J* = 11.7 Hz), 4.55 (d, 1H, *J* = 11.4 Hz), 4.45 (d, 1H, *J* = 11.9 Hz), 4.37 (d, 1H, *J* = 11.9 Hz), 4.26 (dd, 1H, *J* = 8.9 Hz, 5.7 Hz), 4.11 (ddd, 1H, *J* = 13.6 Hz, 5.7 Hz, 3.2 Hz), 4.06 (dd, 1H, *J* = 9.8 Hz, 5.9 Hz), 3.96 (t, 3H, *J* = 6.4 Hz), 3.93–3.91 (m, 1H), 3.72 (dd, 1H, *J* = 9.8 Hz, 2.8 Hz), 3.57 (s, 3H), 3.5–3.4 (m, 2H), 1.75–1.55 (m, 2H), 1.55–1.5 (m, 1H), 1.40 (s, 3H), 1.32 (s, 3H), 1.3–1.1 (m, 5H), 0.81 (t, 3H, *J* = 6.8 Hz).
14. (a) Soucy, R. L.; Kozhinov, D.; Behar, V. *J. Org. Chem.* **2002**, *67*, 1947–1952; (b) Shimada, K.; Kaburagi, Y.; Fukuyama, T. *J. Am. Chem. Soc.* **2003**, *125*, 4048–4049; (c) Tamura, Y.; Annoura, H.; Fuji, M.; Yoshida, T.;

Takeuchi, R.; Fujioka, H. *Chem. Pharm. Bull.* **1987**, *35*, 4736–4746; (d) Reez, M. T. *Angew. Chem., Int. Ed. Engl.* **1984**, *23*, 556–569.

15. The total chemical yield of **10a,b** was decreased to 39% with a similar diastereomeric ratio when the magnesium acetylide of **5** was used in this reaction. The zinc acetylide derived from **5** produced only a trace of **10a,b**.
16. Data for **2b**: $[\alpha]_D^{28}$ +9.3 (*c* 0.10, pyridine); ^{1}H NMR (400 MHz, pyridine-d_5): δ 8.45 (d, 1H J = 7.3 Hz), 5.2–5.05 (m, 1H), 4.74 (dd, 1H, J = 8.9 Hz, 5.4 Hz), 4.6–4.45 (m, 3H), 4.37 (dd, 1H, J = 11.2 Hz, 4.6 Hz), 4.25 (dd, 1H, J = 8.9 Hz, 3.4 Hz), 4.25–4.15 (m, 3H), 2.8–2.65 (m, 1H), 2.65–2.52 (m, 1H), 2.52–2.38 (m, 2H), 2.38–2.15 (m, 3H), 1.95–1.8 (m, 4H), 1.75–1.55 (m, 1H), 1.45–1.1 (m, 44H), 0.87 (t, 3H, J = 6.6 Hz), 0.81 (t, 3H, J = 7.0 Hz); HR-FABMS (*m/z*) $[M+H]^+$ calculated for $C_{40}H_{80}NO_8$, 702.5884, found 702.5853.
17. The effect of **2b** in several animal models of autoimmune disease is currently under investigation and will be reported elsewhere.

NKT Cells Are Critical for the Initiation of an Inflammatory Bowel Response against *Toxoplasma gondii*[1]

Catherine Ronet,* Sylvie Darche,* Maria Leite de Moraes,† Sachiko Miyake,‡ Takashi Yamamura,‡ Jacques A. Louis,* Lloyd H. Kasper,[2§] and Dominique Buzoni-Gatel[2,3]*

We demonstrated in this study the critical role of NKT cells in the lethal ileitis induced in C57BL/6 mice after infection with *Toxoplasma gondii*. This intestinal inflammation is caused by overproduction of IFN-γ in the lamina propria. The implication of NKT cells was confirmed by the observation that NKT cell-deficient mice (Jα281$^{-/-}$) are more resistant than C57BL/6 mice to the development of lethal ileitis. Jα281$^{-/-}$ mice failed to overexpress IFN-γ in the intestine early after infection. This detrimental effect of NKT cells is blocked by treatment with α-galactosylceramide, which prevents death in C57BL/6, but not in Jα281$^{-/-}$, mice. This protective effect is characterized by a shift in cytokine production by NKT cells toward a Th2 profile and correlates with an increased number of mesenteric Foxp3 lymphocytes. Using chimeric mice in which only NKT cells are deficient in the IL-10 gene and mice treated with anti-CD25 mAb, we identified regulatory T cells as the source of the IL-10 required for manifestation of the protective effect of α-galactosylceramide treatment. Our results highlight the participation of NKT cells in the parasite clearance by shifting the cytokine profile toward a Th1 pattern and simultaneously to immunopathological manifestation when this Th1 immune response remains uncontrolled. ***The Journal of Immunology*****, 2005, 175: 899–908.**

Natural killer T cells represent a minor subset of T lymphocytes that share receptor structures with conventional T cells and NK cells (1, 2). Murine NKT cells express intermediate levels of a TCR using a semi-invariant Vα14-Jα281 TCR α-chain paired with Vβ8, -7, or -2 TCR β-chain together with NK cell receptors (NKR-P1, Ly-49, and NK1.1 in C57BL/6 mice) (3, 4). These cells are located mainly in the liver, spleen, thymus, and bone marrow and recognize Ag in the context of the monomorphic CD1d Ag-presenting molecule (5, 6). CD1d and the invariant TCR α-chain are essential for the normal development of NKT cells (7). CD1 molecules present hydrophobic lipid Ags (8), and the marine sponge derived glycolipid, commonly referred to as α-galactosylceramide (α-GalCer),[4] was identified as a potent stimulatory factor for NKT cells (9).

A potential role of NKT cells in the regulation of immune responses has been hypothesized because of their capacity to rapidly release large amounts of IL-4 and IFN-γ upon activation (10). NKT cells play crucial roles in various immune responses, including antitumor, autoimmune, and antimicrobial immune responses (1, 11). Within hours of TCR engagement, CD1d-reactive T cells produce Th1 and/or Th2 cytokines (9, 11, 12) by a mechanism not yet identified that can influence other immune cells, such as conventional T (13–15), NK cells (16), and dendritic cells (DC) (17). NKT cell-derived Th1 cytokines (such as IFN-γ) are important in the initiation of the antitumor immune response, whereas NKT cell-derived Th2 cytokines (IL-4 and IL-10) are involved in down-regulation of the autoimmune response (18). When stimulated with α-GalCer, NKT cells exhibit the ability to proliferate and to produce both Th1 and Th2 cytokines (9, 19). However administration of α-GalCer at the time of priming of mice with Ag results in the generation of only Ag-specific Th2 cells. Thus, α-GalCer might be useful for modulating the immune response toward a Th2 phenotype (12).

Recent evidence suggests that NKT cells are important in the host/pathogen immune response, including cytotoxicity, Ab production, and regulation of Th1/Th2 differentiation. NKT cells have been shown to participate in the immune response to a range of different infectious agents, including *Listeria*, *Mycobacteria*, *Salmonella*, *Plasmodium*, viral hepatitis (20, 21), HIV (22), and even *Toxoplasma gondii* (23). *T. gondii* is an obligate intracellular parasite acquired by oral ingestion of tissue cysts containing either bradyzoites or sporozoites from contaminated soil. It has been observed that after oral infection with tissue cysts, the intestinal epithelial and lamina propria cells are invaded by the parasites. Parasite infection induces a strongly biased Th1 response in the gut that displays a dual effect. IFN-γ produced by the CD4 T cells from the lamina propria (24) limits parasite replication, conferring resistance in mice in certain inbred strains. However, in C57BL/6 (B6) mice, an overwhelming IFN-γ production leads to a lethal acute ileitis within 10 days after oral infection. This *Toxoplasma*-induced intestinal disease shares histological and immunological similarities with human inflammatory bowel disease, such as

*Department of Parasitology, Unit of Early Responses to Intracellular Parasites and Immunopathology, Institut Pasteur-Institut National de la Recherche Agronomique, Paris, France; †Centre National de la Recherche Scientifique, Unité Mixte de Recherche, University René Descartes, Paris V, Hôpital Necker, Paris, France; ‡Department of Immunology, National Institute of Neuroscience, National Center of Neurology and Psychiatry, Tokyo, Japan; and §Departments of Medicine and Microbiology/Immunology, Dartmouth Medial School, Lebanon, NH 03756

Received for publication December 21, 2004. Accepted for publication May 7, 2005.

The costs of publication of this article were defrayed in part by the payment of page charges. This article must therefore be hereby marked *advertisement* in accordance with 18 U.S.C. Section 1734 solely to indicate this fact.

[1] C.R. was the recipient of fellowships from the Association Francois Aupetit and the Joshui/Institut Pasteur Foundation. This work was carried out in the Unit of Early Responses to Intracellular Parasites and Immunopathology and was supported by the Pasteur Institute, the Institut National de la Recherche Agronomique, the Fondation pour la Recherche Médicale. Partial support for this work was provided by National Institutes of Health Grant AI19613.

[2] L.H.K. and D.B.-G. share senior authorship.

[3] Address correspondence and reprint requests to Dr. Dominique Buzoni-Gatel, Department of Parasitology, Unit of Early Responses to Intracellular Parasites and Immunopathology, Institut Pasteur-Institut National de la Recherche Agronomique, 25 rue du Dr Roux, 75724 Paris Cedex 15, France. E-mail address: buzoni@pasteur.fr

[4] Abbreviations used in this paper: α-GalCer, α-galactosylceramide; DC, dendritic cell; IEL, intraepithelial lymphocyte; LPL, lamina propria lymphocyte; MLN, mesenteric lymph node; SAG1, surface Ag-1.

0022-1767/05/$02.00

Crohn's disease. The regulation of this inflammatory process requires a delicate homeostatic balance that is influenced by either a Th1 or Th2 response.

In this report the role of NKT cells in the initiation of the inflammatory process in response to oral infection with *T. gondii* was evaluated. Our findings suggest a potentially critical role for these early responder cells in the initiation and regulation of the lethal inflammatory process.

Materials and Methods

Mice and parasites

Female, 8- to 10-wk-old, inbred B6 mice and CBA were obtained from IFFA-Credo. Mice were housed under approved conditions of the Animal Research Facility at Institut Pasteur. IL-$10^{-/-}$ mice were supplied by Dr. Bandeira (Institut Pasteur, Paris, France). We were provided with Jα281$^{-/-}$ mice by Dr. M. Taniguchi (Riken Research Center for Allergy and Immunology, Yokohama, Japan) (9), Vα14Tg mice by Dr. A. Lehuen (Institut National de la Santé et de la Recherche Médicale, Paris, France) (25), actin-GFP mice by Dr. M. Okabe (Genome Information Research Center, Osaka University, Osaka, Japan) (26), and CD1$^{-/-}$ mice by Dr. L. Van Kaer (Vanderbilt University School of Medicine, Nashville, TN) (7). All the genetically modified strains were on a B6 genetic background. 76K strain cysts isolated from the brains of chronically infected CBA mice were used for in vivo studies. Mice were infected orally by intragastric gavage of 35 cysts, a lethal condition for B6 wild-type mice as described previously (27). After infection, mortality was evaluated, and morbidity was estimated by the percentage of weight loss compared with the initial weight.

Treatment with α-GalCer, anti-CD25, or anti IL-4 Abs

α-GalCer was kept dissolved in PBS buffer containing 20% DMSO at 220 μg/ml as a stock solution. Mice received a single i.p. injection of 5 mg of α-GalCer the day before infection by *T. gondii*. Control mice received an i.p. injection of PBS/20% DMSO, which has no influence on the course of *T. gondii* infection.

Neutralization of IL-4 was conducted by injecting i.p. 1 mg of anti-IL-4 (11B11; provided by Dr. P. Launois, World Health Organization Immunology Research and Training Center, Institute of Biochemistry, Epalinges, Switzerland) mAb 24 h before α-GalCer treatment and 48 h before infection. Control mice were treated with rat IgG Abs (Sigma-Aldrich).

Mice were depleted of CD25$^+$ cells by i.p. administration of 0.5 mg of anti-CD25 (PC61; provided by Dr. R. J. Noelle, Dartmouth Medical School, Lebanon, NH) mAb. Three days after the treatment, the efficiency of CD25$^+$ cell depletion was controlled in peripheral blood by FACS analysis. The CD25$^+$ cell depletion remained stable over 15 days. Control mice were treated with a mouse IgD1 isotype Ab (MOPC31C k; BD Pharmingen).

Cell purification

Lamina propria. The method used to isolate intestinal lamina propria lymphocytes (LPLs) was modified as described previously (24). After dissection and removal of Peyer's patches, the sectioned intestines were incubated in PBS-3 mM EDTA at 37°C and 5% CO_2 (four times, 20 min each time). Then intestinal pieces were incubated at 37°C in RPMI 1640-5% FCS with Liberase (0.14 Wunch units/ml; Roche) and DNase (10 U/ml; Sigma-Aldrich). After 45 min, the digested suspension containing LPLs was filtered on a cell strainer and washed twice, and the pellet was submitted to a Percoll gradient to isolate the lymphocytes. Total cells were resuspended in a 80% isotonic Percoll solution (Pharmacia Biotech) and overlaid with a 40% isotonic Percoll solution. Centrifugation for 30 min at 3000 rpm resulted in concentration of mononuclear cells at the 40–80% interface. The collected cells were washed once with PBS supplemented with 2% FCS. The purity of the LPL population was assessed by the relative percentage of B cells (>50%), CD4 T cells (~20%), CD8 T (<3%) cells, and enterocytes (<5%).

Intraepithelial lymphocytes (IELs). IELs were isolated as previously described (28). Briefly, the small intestine was flushed with PBS and divided longitudinally after removal of Peyers's patches. The mucosae were scraped, dissociated by mechanical disruption, in RPMI 1640 containing 4% FCS and 1 mmol/L DTT. After passage over a glass-wool column, the lymphocytes were separated by Percoll as described for LPLs. The purity of IEL population was assessed by the relative percentages of B cells (<2%), CD4 T cells (<10%), CD8 T cells (>80%), and enterocytes (<5%).

Mesenteric lymph node (MLN) and spleen. MLN and spleen were dissociated and freed of connective tissue by filtration (70 μm). Unless otherwise stated, each mouse was analyzed individually.

Liver. Single-cell suspensions were obtained from liver as described previously by us (29).

Cytometric analysis

FACS analysis of NKT cells. Single-cell suspensions were first incubated 10 min with an anti-FcγRII/III mAb (Fcblock, 2.4G2; BD Pharmingen), followed by a 1-h exposure to CD1d/α-GalCer tetramer-allophycocyanin under agitation at 4°C. CD1d/α-GalCer tetramers were prepared as described by Matsuda et al. (30). After two washes, other cell surface stainings were performed with the following Abs: anti-TCRβ (H57-597), anti-CD4 (RM4-5), anti-CD8 (53-6.7), anti-NK1.1 (PK136), anti-CD25 (C363 16A), anti-CD45RB (7D4), and anti-CD5 (BD Biosciences). PerCP-streptavidin and CyChrome-streptavidin were purchased from BD Biosciences. Cells were analyzed in PBS containing 2% FCS using a FACSCalibur flow cytometer and CellQuest software (BD Biosciences).

Cell sorting. NKT cells stained with the tetramer were magnetically sorted. After tetramer CD1d/α-GalCer-allophycocyanin staining, cells suspensions were incubated for 15 min in PBS/2% FCS/2 mM EDTA at 4°C with anti-allophycocyanin beads as described by the provider (Miltenyi Biotec). After washing and filtration, samples were run on AutoMACS (Miltenyi Biotec). Purity was controlled by cytometric analysis, and the sorted cells were frozen until molecular biology analysis.

For the reconstitution experiment, NKT from the liver and the spleen of actin-GFP mice were sorted with both anti-CD5 biotin (53-7.3), and anti-NK1.1-PE (PK136) mAbs and streptavidin-allophycocyanin using a MoFlo (DakoCytomation). Purified NKT-GFP$^+$ cells were collected in RPMI 1640 supplemented with 10% FCS. The purity of the sorted NKT-GFP cells was found to exceed 97%.

Adoptive transfer of NKT-GFP$^+$ cells. Highly purified NKT cells (1×10^6) were injected i.v. into Jα281$^{-/-}$ mice. At the same time these mice were treated with 5 μg of α-GalCer i.p. One day later, NKT cells were transferred, and α-GalCer-treated mice were infected.

Histological examination

Histopathology and morphometric analysis. Intestines were immediately fixed in buffered 10% formalin after dissection. Then they were embedded, sectioned, and stained with H&E for histological examination. Inflammation was scored by the ratio of the length/thickness of the villi (mean of 20 measures for a total of four different fields).

Confocal microscopic examination. Intestinal and hepatic samples from NKT-GFP-transferred mice were microscopically examined. On day 7 after infection mice were scarified, and samples from intestines and livers were incubated for 24 h in paraformaldehyde (4%) and saccharose (30%). Then tissues were frozen in liquid nitrogen using OCT embedding compound (Sakura). Frozen sections (10 μm) were cut on a microtome HM 505 cryostat (Microcom Laboratory), fixed with PBS/paraformaldehyde (4%), permeabilized by PBS/Triton (0.1%), contrastained with rhodamine phallodin (Molecular Probes), and mounted with Vectashield (Vector Laboratories). Preparations were analyzed with fluorescent microscope Axioplan 2 imaging coupled with an ApoTome system (Zeiss). GFP-NKT cell trafficking was also assessed by FACS analysis performed on day 7 after infection with cell suspensions obtained from lamina propria and livers.

Bone marrow chimeric mice

Recipient mice were lethally irradiated (900 rad) with a ^{137}Ce source. Then they received i.v. bone marrow cells (1×10^7) recovered from femurs and tibias of donor mice. To generate mice with only NKT cells devoid of the IL-10 gene, a mix (50/50%) of bone marrow cells from Jα281$^{-/-}$ mice and IL-$10^{-/-}$ mice was prepared. Control mice received cells from B6, Jα281$^{-/-}$ or IL-$10^{-/-}$ mice alone. Six weeks after reconstitution, mice were bled, and the presence of CD4$^+$, CD19$^+$ (1D3), and CD11c$^+$ (HL3) cells was monitored by flow cytometric analysis. Reconstitution with NKT was assessed (two mice per group) by staining the CD1d/α-GalCer-allophycocyanin tetramer cell suspensions obtained from the liver and lamina propria of the chimera. Chimeric mice were then infected. At different times after infection, LPLs and MLN cell suspensions were phenotyped by FACS analysis. Morbidity was evaluated daily by recording the weight loss, and mortality was also recorded.

RNA extraction, cDNA preparation, and real-time RT-PCR

Tissue samples from intestines and purified cells were kept frozen (−70°C) until mRNA extraction. Specimens were disrupted in a Polytron (Brinkmann Instruments) and homogenized in 350 ml of RLT buffer (Qiagen).

RNA extraction and cDNA preparation were conducted following standard procedures using oligo(dT)$_{17}$ primers, and 10 U of avian myeloblastosis virus reverse transcriptase. Quantitative PCR was performed with the GeneAmp 7000 (Applied Biosystems) as indicated by the supplier. Primers and probes for the quantitative PCR assay of cytokines and actin were designed as previously described (31). Foxp3 mRNA were analyzed with applied assay on demand n°Mm00475156_m1 (Applied Biosystems).

Parasite burden

DNA was extracted from the different organ samples using a DNAeasy kit (Qiagen). The *Toxoplasma* B1 gene was amplified by quantitative real-time PCR (32). Parasite titration by real-time PCR was performed with the GeneAmp 7000 (Applied Biosystems). The standard curve established from the serial 10-fold dilutions of *T. gondii* DNA of parasite concentrations ranging from 1×10^6 to 10, showed linearity over a 6-log concentration range and was included in each amplification run. At different time points after infection, tissue samples were recovered, and their DNA were extracted with the DNeasy Tissue Kit (Qiagen). For each sample, parasite count was calculated by interpolation from the standard curve. The parasite burden was expressed as the number of parasites per milligram of samples. Cerebral parasite burden was evaluated by enumeration of the cysts on day 30 after infection.

Statistical analysis

Results are expressed as the mean ± SD. Statistical differences between groups were analyzed using Student's t test. A value of $p < 0.05$ was considered significant.

Results

Presence of NKT cell in the lamina propria

The presence of the NKT lymphocyte subpopulation within the gut was demonstrated by FACS analysis using the CD1d/α-GalCer tetramers. In the lamina propria of naive B6 mice, 2% of the mononuclear cells (LPLs) were detected (Fig. 1*A*). NKT cells were not detected in cell suspensions from the IEL compartment (Fig. 1*A*). Seventy to 80% of the tetramer-positive cells were CD4$^+$; the remainder were CD4$^-$CD8$^-$ double negative. During the days following infection, a decrease in the number of tetramer-positive cells was observed (Fig. 1*B*) that could be due to TCR downregulation. Serial time point phenotyping after infection demonstrated that all NKT cells were CD25$^-$. To assess NKT cell trafficking into the intestine after infection, Jα281$^{-/-}$ mice were transferred with NKT-GFP$^+$ cells (1×10^6) highly purified from the livers of GFP transgenic mice on the basis of CD5 and NK1.1 expression (Fig. 1*D*, *a*). At 7 days after infection, GFP$^+$ cells were found in cell suspension obtained from the liver (Fig. 1*D*, *b*) and lamina propria (Fig. 1*D*, *c*) of the transferred mice. Histological examination by confocal microscopy revealed that within the liver, NKT-GFP$^+$ cells were distributed among hepatocytes near the sinusoids (Fig. 1*E*). Within the gut, NKT-GFP$^+$ cells were always

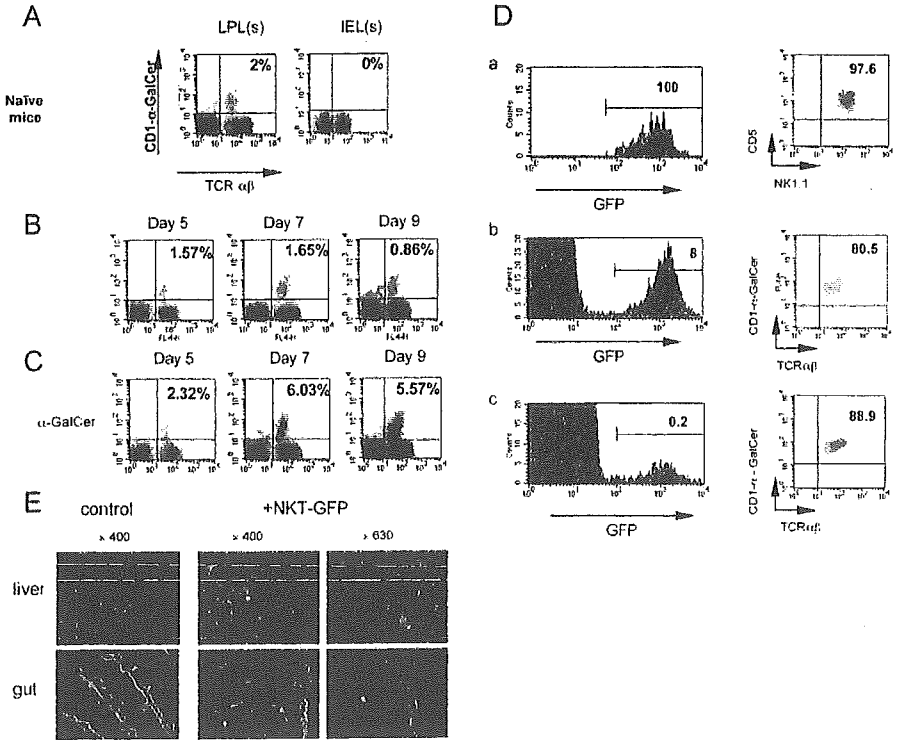

FIGURE 1. NKT cells are present in the lamina propria compartment. *A*, Representative FACS profiles showing Vα14 CD1d/α-GalCer$^+$ TCRαβ$^+$ cells obtained from LPL and IEL suspension from naive mice. The numbers indicate the proportion of tetramer-positive T cells in the lymphocyte gate. This analysis was performed with five mice and was repeated twice. *B*, Representative FACS profiles showing Vα14 CD1d/α-GalCer$^+$TCRαβ$^+$ cells obtained from LPL suspensions of mice at different times after infection. This analysis was performed with five mice individually and was repeated twice. *C*, Representative FACS profiles showing Vα14 CD1d/α-GalCer$^+$TCRαβ$^+$ cells obtained from LPL suspensions of α-GalCer-treated mice at different times after infection. This analysis was performed with five mice and was repeated twice. *D*, NKT cell populations from actin-GFP mice were purified on the basis of GFP, CD5, and NK1.1 (PE) expression and were positively selected with magnetic beads directed against PE. *D*, *a*, Purity of the selected NKT cell population. One million purified NKT cells were injected i.v. into Jα281$^{-/-}$ mice. The following day, these mice were infected with *T. gondii*. On day 7 after the adoptive transfer, Jα281$^{-/-}$ recipients showed a significant presence of GFP$^+$ cells in the liver (*b*) and lamina propria (*c*) cell suspension, which are almost all NKT cells as revealed by CD1d/α-GalCer$^+$ staining after gating on GFP$^+$ cells. Four mice were adoptively transferred with NKT-GFP cells, requiring 24 GFP transgenic donor mice. *E*, GFP$^+$ NKT cells were detected in paraformaldehyde-fixed cryosections of liver and intestine from Jα281$^{-/-}$ recipient mice (the control was sections from naive Jα281$^{-/-}$ mice). Actin filaments were stained in red with rhodamine phallodin to visualize the organ structure. Original magnifications: ×400 and ×630. The pictures shown are representative of observations made with the four NKT-GFP cell recipient mice.

localized in the lamina propria and were never associated with the IEL compartment (Fig. 1*E*). These data indicated that NKT cells traffic to the intestine, where they localize within the lamina propria.

Importance of NKT cells in the development of acute inflammatory ileitis in B6 mice

The involvement of NKT cells in the initiation of the intestinal inflammation after oral infection with *T. gondii* was investigated by comparing the outcome of the infection in wild-type B6 mice and mice genetically deficient in NKT cells (Jα281$^{-/-}$ mice). As expected, all control B6 mice died within 7–10 days of severe ileitis after oral challenge with 35 cysts (Fig. 2*A*). The intestinal inflammation and subsequent morphological changes were characterized by cellular infiltration within the lamina propria; short, thickened villi; and patchy transluminal necrosis. In contrast, Jα281$^{-/-}$ mice developed a less severe disease (Fig. 2*B*) associated with 1) a decrease in the length/thickness ratio of the villi compared with B6 infected mice (Fig. 2*C*), 2) a significantly delayed time of death, and 3) a decrease in the mortality rate compared with B6 mice (Fig. 2*A*). This outcome was not parasite dose dependent, as determined using a lower infectious dose of cysts (10 cysts/mouse) in which all the Jα281$^{-/-}$ mice survived, whereas 25% of the B6 died (Fig. 2*D*). These results indicate that the absence of NKT cells correlates with a more resistant phenotype. However, CD1d$^{-/-}$ mice were even more susceptible than B6 mice (Fig. 2*A*). In addition to NKT depletion, regulatory cells, such as IEL and B cells, are also reduced in CD1d$^{-/-}$ mice (33, 34).

To further explore the potential role of NKT cells in the inflammatory process, mice that overexpressed NKT cells (Vα14Tg mice) were infected. Both B6 and Vα14Tg mice died within 7–10 days when infected with 35 cysts (Fig. 2*A*). However, in the experiment using a lower dose of cysts (10 cysts/mouse), all the Vα14Tg mice died, whereas only 25% of the B6 mice died (Fig. 2*D*). These data confirm that NKT cells are important in the innate host response to oral parasite infection and are involved in disease susceptibility.

NKT cell activation correlates with intestinal IFN-γ production after T. gondii *infection*

IFN-γ is an important cytokine in mediating host defense against *T. gondii* infection. It limits parasite replication, but, at the same time, if overproduced, it leads to the development of overwhelming intestinal inflammation. Therefore, because NKT cell-deficient

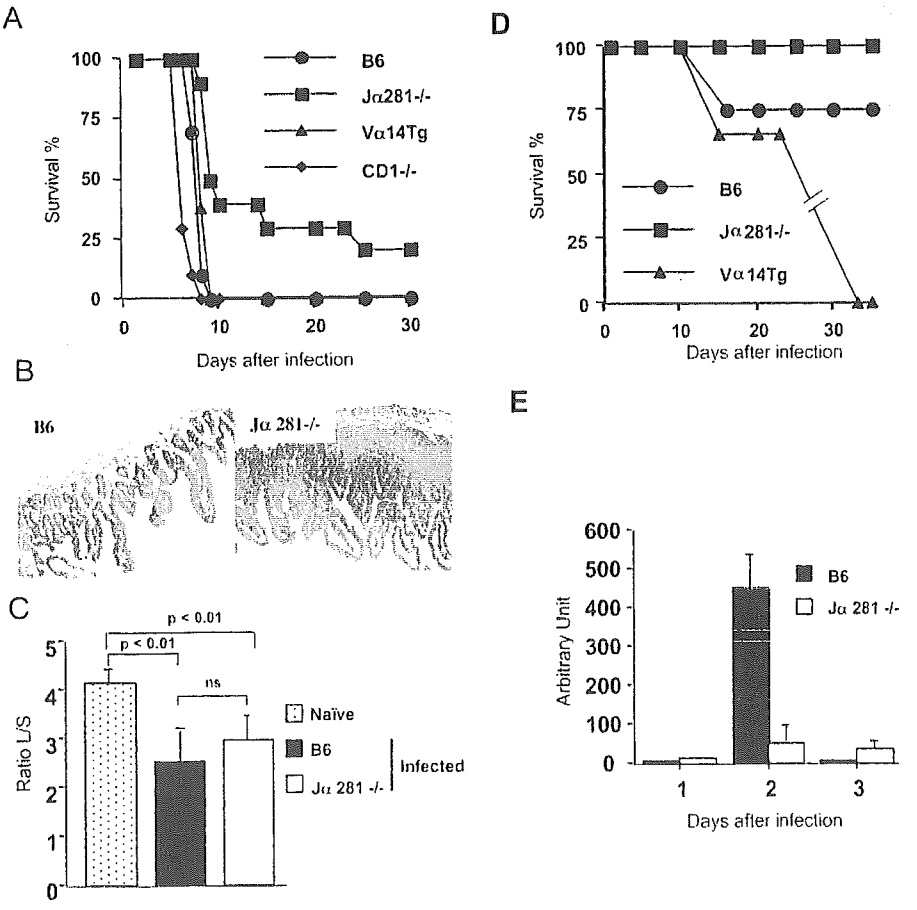

FIGURE 2. NKT cells are involved in the development of acute inflammatory ileitis in B6 mice. *A*, Survival rate of B6, Jα281$^{-/-}$, Vα14Tg, and CD1d$^{-/-}$ mice after challenge with 35 cysts of *T. gondii* (n = 10/group). Data are representative of three independent experiments with similar results. *B*, Intestinal H&E histology from B6 and Jα281$^{-/-}$ mice on day 7 after challenge (magnification, ×200). Results are representative of two independent experiments performed with four mice each time. *C*, Intestinal lesions from B6 and Jα281$^{-/-}$ on day 7 after challenge were scored as the ratio of the villi length to its thickness. These data were the mean of 20 measures obtained with four different fields and repeated with two mice per group. *D*, Survival rate of B6, Jα281$^{-/-}$, Vα14Tg after challenge with 10 cysts of *T. gondii* (n = 5/group). Data are representative of two independent experiments with similar results. *E*, Early IFN-γ mRNA expression in the intestine after infection is dependant upon the presence of NKT cells. Samples from the ileum of B6 and Jα281$^{-/-}$ mice were analyzed for mRNA expression of IFN-γ by real-time RT-PCR. Results are expressed as the fold increase relative to noninfected control mice after normalization with the housekeeping gene. The mean ± SD were calculated from two samples from two mice. Results are representative of three independent experiments.

mice ($J\alpha281^{-/-}$) were more resistant to the development of lethal ileitis after *T. gondii* infection, the expression of IFN-γ in their intestines was measured at different times after oral challenge with the cysts. Between days 2 and 3 after infection, IFN-γ mRNA expression peaked in the intestine of B6 mice, and there was a significant difference in IFN-γ mRNA expression between B6 mice and $J\alpha281^{-/-}$ mice. By quantitative RT-PCR, the level of mRNA expression in B6 mice was 9–10 times higher than that in $J\alpha281^{-/-}$ mice (Fig. 2*E*). Over time, inflammatory cytokine production in $J\alpha281^{-/-}$ mice may increase, contributing in the delayed time to death due to lethal intestinal inflammation. The lack of early production of IFN-γ might also explain the 2-fold increase in parasite burden in $J\alpha281^{-/-}$ mice on day 8 after infection. These findings strongly suggest that NKT cell activation after oral infection with *T. gondii* is associated with early initiation of the Th1 process observed in the intestines of B6 mice.

Treatment with α-GalCer protects against the development of lethal ileitis

Because α-GalCer can influence the nature of the cytokines produced by NKT cells and consequently the orientation of the adaptative Th response, mice were treated with α-GalCer the day before infection. Up to 30 days after infection, this treatment prevented death in both B6 (100%) and V14αTg mice overexpressing NKT cells (80%; Fig. 3*A*). Histological examination performed on day 7 after infection revealed that treatment with α-GalCer interfered with the development of ileitis (Fig. 3, *B* and *C*). In addition, B6 mice treated with α-GalCer exhibited less weight loss compared with untreated infected controls (Fig. 3*D*). To assess the cell population targeted by α-GalCer treatment, NKT-deficient mice ($J\alpha281^{-/-}$) were treated with α-GalCer the day before infection. This treatment had no effect on the infection outcome in $J\alpha281^{-/-}$ mice (Fig. 3*A*), as attested by the early time of death and the histological damages observed in treated mice (Fig. 3*B*). These observations strongly suggest that α-GalCer modulates the functional abilities of NKT cells. Treatment with α-GalCer was not directly toxic to the parasite, because there was no difference in parasite burden in $J\alpha281^{-/-}$ mice treated or not treated on day 30 after infection (data not shown). Treatment with α-GalCer 2 days after infection failed to impact the development of the hyperinflammatory response in small intestine.

Treatment with α-GalCer induces preferential production of IL-4 and IL-10 in T. gondii*-infected mice*

One of the consequences of α-GalCer treatment was the increase in the number of NKT cells in the lamina propria of infected mice (Fig. 1*C*). The production of selected cytokines in the whole intestine of α-GalCer-treated mice was monitored by quantitative RT-PCR. A significant increase in IL-10 (180-fold) and IL-4 (80-fold) mRNA expression was observed in the intestines of α-GalCer-treated mice on days 3 and 5, respectively, after infection. In contrast, no increase in IL-13 mRNA expression in the whole intestine of α-GalCer-treated mice was measured at serial time points after infection. mRNA for IFN-γ was also significantly decreased (10-fold) in α-GalCer-treated mice (data not shown). This result demonstrated a shift in cytokine production toward a Th2-like profile after treatment with α-GalCer and infection and a decline in the Th1-like immune response. To better assess the contribution of intestinal NKT cells in this shift, α-GalCer-treated mice and untreated control mice were killed on day 8 after infection, and NKT cells were purified from the lamina propria (Fig. 4*A*). As shown in Fig. 4*A*, the purity of the sorted population was

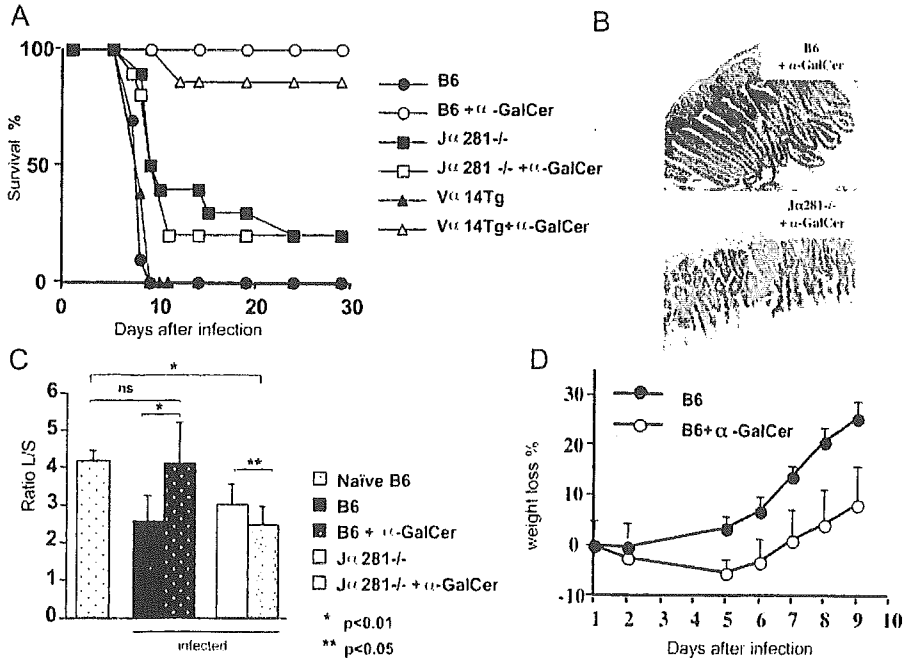

FIGURE 3. α-GalCer treatment protects the infected mice against the development of lethal ileitis. *A*, Survival rates of B6, $J\alpha281^{-/-}$, and $V\alpha14Tg$ mice after i.p. administration of 5 μg of α-GalCer the day before challenge with *T. gondii* (n = 10/group). Results are representative of two independent experiments. *B*, Intestinal H&E histology of α-GalCer-treated or untreated mice on day 7 after infection (magnification, ×200). *C*, Intestinal lesions in α-GalCer-treated or untreated mice on day 7 after infection were scored as the ratio of the villi length to its thickness. These data were the mean of 20 measures obtained with four different fields and repeated with two mice per group. *D*, B6 mice treated with α-GalCer exhibited only mild weight loss compared with untreated infected controls. Infected B6 mice treated, or not, with α-GalCer were weighed daily. Weight loss is expressed as a percentage of the animal's initial weight.

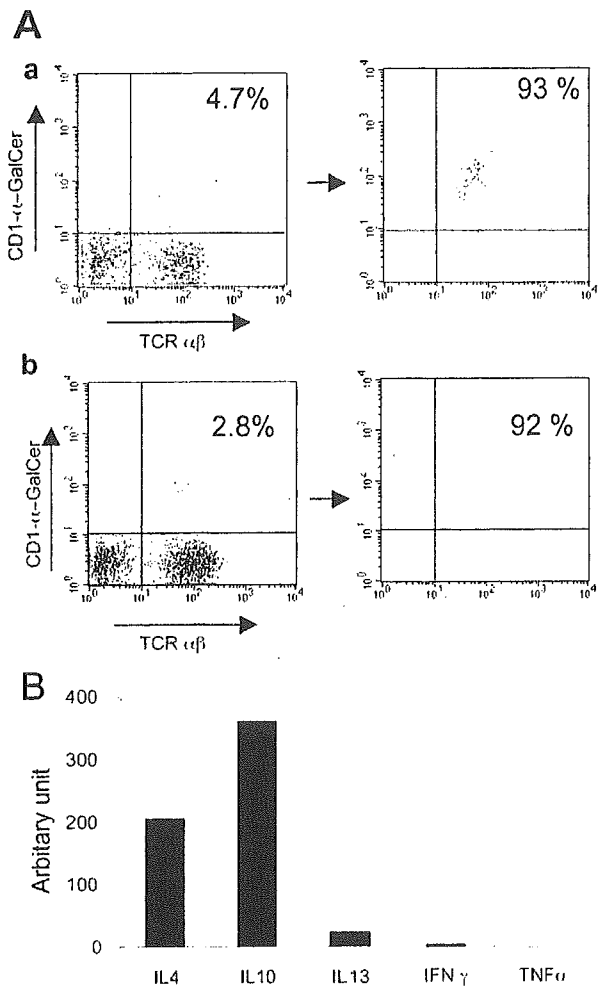

FIGURE 4. NKT cells produce Th2 cytokine after α-GalCer administration and *T. gondii* infection. *A*, NKT cell populations were isolated from the lamina propria of mice treated (*a*) or not treated (*b*; two mice per group) with α-GalCer on day 8 after infection. The cells were then purified on the basis of CD1d/α-GalCer tetramer staining using anti-allophycocyanin magnetic beads. The purity of sorted cells was confirmed by FACS analysis. This experiment was repeated twice. *B*, Purified NKT cells were analyzed for mRNA expression of Th1 and Th2 cytokines by real-time RT-PCR. Results are expressed as the relative increase in the cytokines in NKT cells from treated mice compared with the untreated NKT cells after normalization with the housekeeping gene. Results are representative of two independent experiments.

>90% in both α-GalCer-treated (Fig. 4*A*, *a*) and untreated (Fig. 4*A*, *b*) animals. The mRNA production of different cytokines by the purified NKT cell population was measured by RT-PCR. The results are expressed as the relative increase or decrease in mRNA expression for different cytokines in NKT cells isolated from α-GalCer-treated mice compared with control infected, but untreated, mice. Compared with controls, IL-10, IL-4, and IL-13 mRNA expressions were increased in the NKT cell population isolated on day 8 from mice treated with α-GalCer and infected (Fig. 4*B*). These data indicate that treatment with α-GalCer shifts the NKT cell cytokine pattern to a Th2-like profile.

The production of IL-10 and IL-4 by NKT cells stimulated with α-GalCer was increased in the intestines of treated mice. In contrast, IL-13 production by NKT cells after treatment with α-GalCer did not lead to an increase in this cytokine in the whole intestine throughout the serial time points after infection.

Role of IL-4 in protection against T. gondii*-induced death*

The contribution of IL-4 production associated with α-GalCer treatment to interference with the induction of *T. gondii*-induced death was evaluated by a series of experiments using blocking Ab. Blocking of IL-4 the day before α-GalCer treatment partially reversed its beneficial effect, as shown by a 50% survival rate compared with 100% survival of mice in the α-GalCer alone-treated group (Fig. 5*A*). These observations suggest a partial role for IL-4 in the protection induced by α-GalCer in this model.

Critical role of IL-10 in protection against T. gondii*-induced ileitis*

The contribution of IL-10 production associated with α-GalCer treatment in interfering with the induction of *T. gondii*-induced death was evaluated using genetically deficient and chimeric mice. Strikingly α-GalCer treatment had no beneficial effect on protection in IL-10$^{-/-}$ mice (Fig. 5*B*). These observations suggest a pivotal role for IL-10.

To determine whether IL-10 produced by NKT cells was sufficient to suppress lethal intestinal inflammatory lesions, double-chimeric mice were generated. B6 mice were irradiated and reconstituted by a 50/50% mix of bone marrow cells from Jα281$^{-/-}$ (NKT cell-deficient) and IL-10$^{-/-}$ mice. After reconstitution, the double-chimeric mice expressed a normal immunological phenotype, except for the NKT cells that were IL-10$^{-/-}$ (NKT IL-10$^{-/-}$). These NKT IL-10$^{-/-}$ chimeric mice and their appropriate controls (B6 mice, Jα281$^{-/-}$ and IL-10$^{-/-}$ mice) were treated with α-GalCer the day before infection. NKT IL-10$^{-/-}$ chimeric mice treated with α-GalCer rapidly lost more weight than α-GalCer-treated B6 mice (Fig. 5*C*), indicating that the lack of IL-10 production by the NKT cells alone conferred greater susceptibility to the infection.

However, in contrast to what was expected, the decreased protective effect of α-GalCer treatment in NKT IL-10$^{-/-}$ chimeric mice did not lead to a significant increase in the mortality rate (80% survival; Fig. 5*D*). These results, demonstrating the complete lack of effect of α-GalCer treatment in IL-10$^{-/-}$ mice (Fig. 5*B*) and a reduced effect of this treatment in NKT IL-10$^{-/-}$ chimeric mice (Fig. 5, *C* and *D*), suggested that other cell types might be the source of the IL-10 that is critical for protection. T regulatory cells (CD4$^+$CD25$^+$) that express the transcription factor FoxP3 and are known as important IL-10 producers were assessed after treatment with α-GalCer and infection. Interestingly, the number of CD4$^+$CD25$^+$ cells from intestines and MLNs were increased on days 6 and 9, respectively (data not shown), after infection, and this correlates with an increased expression of FoxP3 in the intestine on day 6 and in MLNs on day 9 from B6 mice, but not from Jα281$^{-/-}$ mice (Fig. 6*A*). The sorted CD4$^+$CD25$^+$ cell subpopulation exhibited IL-10 mRNA expression (data not shown). Whatever the time after infection and the treatment with or without α-GalCer, the sorted NKT cell population failed to express either FoxP3 or CD25. To better characterize the implication of these T regulatory cell subpopulations to the protective process induced by α-GalCer, the effect of this treatment in mice also treated with blocking anti-CD25 Abs was studied. Treatment with anti-CD25 abrogated the protection (Fig. 6*B*), indicating the crucial role of these cells in the anti-inflammatory process induced by treatment with α-GalCer.